A Dissertation for the Degree of Doctor of Philosophy

The roles of redox homeostasis in prostate cancer depending on the stages of cancer and levels of oxidative stress

전립선 암에서 암의 단계와 산화 스트레스 수준에 따른 산화환원항상성의 역할

By

Ukjin Kim, D.V.M.

February 2020

Department of Veterinary Pathobiology and Preventive Medicine

(Laboratory Animal Medicine)

Graduate School of Seoul National University

The roles of redox homeostasis in prostate cancer

depending on the stages of cancer and levels of oxidative stress

By

Ukjin Kim, D.V.M.

A dissertation submitted to the Graduate School in
Partial fulfillment of the requirement for the degree of
DOCTOR OF PHILOSOPHY

Supervisor: Prof. Jae-Hak Park, D.V.M., Ph.D.

To the Faculty of College of Veterinary Medicine
Department of Veterinary Medicine
Veterinary Pathobiology and Preventive Medicine
(Laboratory Animal Medicine)
The Graduate School of Seoul National University

Ukjin Kim, D.V.M.

February 2020

Dissertation Committee:

Chairman	Seok, Seung Hyeok
Vice Chairman	Park, Jae-Hak
Member	Kang, Kyung-Sun
Member	Ryu, Doug-Young
Member	Kim, C-Yoon

ABSTRACT

The roles of redox homeostasis in prostate cancer depending on the stages of cancer and levels of oxidative stress

Ukjin Kim, D.V.M.

Department of Veterinary Pathobiology and Preventive Medicine

(Laboratory Animal Medicine)

Graduate School of Seoul National University

Supervisor: Prof. Jae-Hak Park, D.V.M., Ph.D.

Prostate cancer is the most diagnosed non-skin cancer in men in developed countries and is a leading cause of cancer-related deaths. Prostate cancer is closely related to age, and several signaling pathways involving reactive oxygen species (ROS), which increase with age, play important roles in the development and progression of cancer. In general, ROS promote cell proliferation, invasion, and metastasis, while inhibiting apoptosis, leading to cancer progression. Therefore, anticancer agents have been reported based on antioxidant effects. However, higher levels of ROS have anti-cancer effects, by causing cell cycle arrest, apoptosis, and necrosis. There is still much to be known about the role of ROS in prostate cancer.

A study in Chapter I reported that phloretin, a polyphenol, induces oxidative stress to inhibit prostate cancer cells, PC3 and DU145. In this study, changes in proliferation, colony formation, and migration after phloretin treatment in human prostate cancer cells PC3 and DU145 were examined. ROS and gene expression were measured. Phloretin increased ROS and suppressed cell proliferation, migration, and colony formation in both cell lines. Additionally, phloretin treatment increased oxidative stress, as demonstrated through lower antioxidant enzymes (catalase, SOD2, Gpx1, Gpx3). In addition, their regulator CISD2 decreased in expression. We also found that increased ROS significantly downregulated multiple components of the Wnt/β-catenin signaling pathway (β-catenin, TCF4, FoxA2, c-Myc) and Twist1. Thus, anticancer activity of phloretin against human prostate cancer cells occurs through generating ROS to influence Wnt/β-catenin signaling. The results of this study suggest that phloretin has a therapeutic effect on prostate cancer *in vitro*, inhibiting the proliferation and migration of cancer cell lines PC3 and DU145. The mechanism of phloretin appears to be increasing ROS production. I recommend phloretin as a promising anticancer therapeutic agent.

Chapter II focuses on drug repurposing to evaluate the anticancer capacity of drugs that have already been approved for other purposes, as a way to discover new drugs. Chapter II reported that the FDA-approved antipsychotic drug, pimozide, inhibits prostate cancer *in vitro* and *in vivo* by inducing oxidative stress in prostate cancer. We examined cell proliferation, colony formation, migration, ROS production, and the expression of antioxidant-related genes after treatment of human prostate cancer PC3 and DU145 cells with pimozide. In addition, histopathology, ROS production, and SOD activity were analyzed after administering pimozide to TRAMP, a transgenic mouse with prostate cancer. Pimozide increased the generation of ROS

in both cell lines and inhibited cell proliferation, migration, and colony formation. Oxidative stress induced by pimozide caused changes in the expression of antioxidant enzymes (SOD1, Prdx6, and Gpx2) and CISD2. Co-treatment with glutathione, an antioxidant, reduced pimozide-induced ROS levels and counteracted the inhibition of cell proliferation. Administration of pimozide to TRAMP mice reduced the progression of prostate cancer with increased ROS generation and decreased SOD activity. These results suggest that the antipsychotic drug, pimozide, has beneficial effects in prostate cancer *in vivo* and *in vitro.* The mechanism of pimozide may be related to augmenting ROS generation. We recommend pimozide as a promising anticancer agent.

Chapters I and II reported that anticancer agents suppress prostate cancer by oxidative stress, with prostate cancer cells and TRAMP mice. Chapter III studied how inherently broken redox homeostasis affects precancerous stage of prostate cancer with genetically modified mice. Glutathione peroxidase 3 (*GPX3*) protects cells from oxidative stress and its reduced expression in human prostate cancer specimens has been reported. We previously reported that down-regulation of *Gpx3* increased prostate cancer in TRAMP mice. We hypothesized that Gpx3 might play an important role in the development of prostatic intraepithelial neoplasia (PIN), a pre-cancer stage of the prostate. The double-knockout mice *Nkx3.1*$^{-/-}$*; Gpx3*$^{+/+,}$ *Nkx3.1*$^{-/-}$*; Gpx3*$^{+/-}$, and *Nkx3.1*$^{-/-}$*; Gpx3*$^{-/-}$ were produced. Randomly divided animals were weighed and genitourinary tract (GUT) weights were measured after euthanasia at 4, 8 and 12 months. The mRNA expression of genes related to oxidative stress and Wnt signaling was analyzed in the prostate. In addition, histopathology, ROS and SOD activities were measured. Down-regulation of *Gpx3* did not significantly affect body weight and GUT weight in *Nkx3.1* knockout mice. The mRNA expression of *Sod3, Nos, Hmox*, and *Cisd2*, which were associated with oxidative stress, were significantly increased

in *Nkx3.1*$^{-/-}$; *Gpx3*$^{-/-}$ mice at 4 months of age, but significantly decreased at 8 months and 12 months. There was no significant change in β-catenin and its target signals associated with Wnt signaling. Increased ROS and decreased SOD activity were observed in *Nkx3.1*$^{-/-}$; *Gpx3*$^{-/-}$ mice at 12 months of age. The histopathologic score and epithelium thickness were increased and lumen area was decreased in *Gpx3* KO mice. The results report for the first time that the antioxidant enzyme *Gpx3* plays a role in inhibiting hyperplasia in the early precancerous PIN stage of the prostate gland *in vivo*.

The roles of redox homeostasis in prostate cancer may depend on the stages of the cancer and the levels of oxidative stress. I observed changes in prostate cancer cell lines, TRAMP mice, and *Nkx3.1; Gpx3* KO mice by inducing oxidative stress, respectively. The treatment of phloretin and pimozide in cancer cell lines or TRAMP mice has been shown to inhibit cancer with oxidative stress. On the contrary, it was confirmed that oxidative stress promoted progression to cancer at the precancerous stage in *Nkx3.1; Gpx3* KO mice. It is necessary to identify and access the roles of redox homeostasis according to the context of cancer. In this dissertation, I suggest that redox homeostasis of prostate cancer is an important target in understanding the biological, physiological and pathological characteristics of prostate cancer and in developing new anticancer strategies.

Keywords: Prostate cancer, Redox homeostasis, Reactive oxygen species (ROS), Anticancer, Gpx3

Student number: 2016-21761

TABLE OF CONTENTS

ABSTRACT ---------- i

TABLE OF CONTENTS ---------- v

LIST OF FIGURES ---------- ix

LIST OF TABLES ---------- xi

LIST OF ABBREVIATION ---------- xii

GENERAL INTRODUCTION ---------- xiii

LITERATURE REVIEW ---------- xv

CHAPTER I

Phloretin inhibits the human prostate cancer cells through the generation of reactive oxygen species ---------- 1

1 INTRODUCTION ---------- 2

2 MATERIALS AND METHODS ---------- 4

2.1 Reagents ---------- 4

2.2 Cell proliferation assay ---------- 4

2.3 Clonogenic assay ---------- 5

2.4 Cell migration assay ---------- 6

2.5 ROS measurement ---------- 6

2.6 Real-time reverse transcription-polymerase chain reaction (PCR) ---------- 6

2.7 Statistical analysis ---------- 8
3 RESULTS ---------- 9
3.1 Phloretin inhibits cell proliferation and colony formation in the PC3 and DU145 cell lines ---------- 9
3.2 Phloretin inhibits migration of PC3 and DU145 cell lines ---------- 11
3.3 Phloretin induces ROS accumulation in PC3 and DU145 cell lines through inhibiting antioxidant enzyme gene expression ---------- 13
3.4 Phloretin downregulates the mRNA levels of Wnt/β-catenin signaling in PC3 and DU145 cell lines ---------- 15
4 DISCUSSION ---------- 17

CHAPTER II

Pimozide Inhibits the Human Prostate Cancer Cells through the Generation of Reactive Oxygen Species ---------- 20

1 INTRODUCTION ---------- 21
2 MATERIALS AND METHODS ---------- 23
2.1 Reagents ---------- 23
2.2 Cell proliferation assay ---------- 23
2.3 Clonogenic assay ---------- 24
2.4 Scratch assay ---------- 24
2.5 ROS measurement in cell ---------- 24
2.6 Real-time reverse transcriptase-polymerase chain reaction (PCR) ---------- 25
2.7 Animals ---------- 25

2.8 Tissue excision and processing ---------- 26
2.9 Histopathological analysis ---------- 27
2.10 ROS measurement in tissue ---------- 27
2.11 SOD assay ---------- 28
2.12 Statistical analysis ---------- 28
3 RESULTS ---------- 29
3.1 Pimozide inhibits cell proliferation and colony formation in the PC3 and DU145 cell lines ---------- 29
3.2 Pimozide inhibits migration of PC3 and DU145 cells ---------- 31
3.3 Pimozide inhibits the proliferation of PC3 and DU145 cells through ROS accumulation, which was inhibited by the antioxidant GSH ---------- 33
3.4 Pimozide inhibits prostate cancer development in TRAMP mice through the generation of ROS ---------- 35
4 DISCUSSION ---------- 38

CHAPTER III

Down regulation of glutathione peroxidase 3 induces ROS and contributed to prostate hyperplasia in *Nkx3.1* knockout mice ---------- 41

1 INTRODUCTION ---------- 42
2 MATERIALS AND METHODS ---------- 44
2.1 Cell cultures ---------- 44
2.2 ROS measurement in cell ---------- 44
2.3 Cell proliferation assay ---------- 45

2.4 Animals and PCR genotyping ---------- 45
2.5 Tissue excision and processing ---------- 46
2.6 Real-time reverse transcriptase-polymerase chain reaction (PCR) ---------- 46
2.7 ROS measurement in prostate tissues ---------- 48
2.8 SOD assay ---------- 48
2.9 Histopathological Analysis ---------- 49
2.10 Statistical analysis ---------- 49
3 RSEULTS ---------- 50
3.1 Oxidative stress promoted proliferation in normal prostate cell RWPE-1 --- 50
3.2 *Gpx3* Knockout did not cause drastic changes in the prostate gland -------- 52
3.3 *Gpx3* Knockout alters the expression of genes associated with oxidative stress, but does not alter Wnt/β-catenin signaling ---------- 54
3.4 *Gpx3* knockout increased ROS production and decreased SOD activity in the prostate ---------- 57
3.5 *Gpx3* knockout increased hyperplasia of the prostate gland ---------- 59
4 DISCUSSION ---------- 61
GENERAL CONCLUSION ---------- 64
REFRENCES ---------- 67
국문 초록 ---------- 81

LIST OF FIGURES

LITERATURE

Figure I Prostate cancer is the most commonly diagnosed cancer in men ---------- xvi

Figure II Roles of ROS in cancer according to ROS level ---------- xviii

Figure III Antioxidant Gpx3 could mediate lung cancer suppression -xxvi

CHAPTER I

Figure 1 The effect of phloretin on cell proliferation ---------- 10

Figure 2 The effect of phloretin on colony formation ---------- 10

Figure 3 The effect of phloretin on migration of PC3 and DU145 --- 12

Figure 4 Phloretin induced generation of ROS in the PC3 and DU145 cell lines ---------- 14

Figure 5 The effect of phloretin on mRNA expression levels of SOD2, CAT, Gpx1, Gpx3 and CISD2 in PC3 and DU145 cells --- 14

Figure 6 The effect of phloretin on mRNA expression levels of Twist1, β-catenin, TCF4, FoxA2, and c-Myc in PC3 and DU145 cells ---------- 16

CHAPTER II

Figure 1 The effect of pimozide on cell proliferation. ---------- 30

Figure 2 The effect of pimozide on migration of PC3 and DU145 --- 32

Figure 3 The effect of pimozide on the prostate cancer cells is related to ROS generation ---------- 34

Figure 4 Effect of pimozide administration on prostate cancer progression in TRAMP mice ---------- 36

Figure 5 Effect of pimozide administration on prostate cancer progression in TRAMP mice ---------- 37

CHAPTER III

Figure 1 Promoted proliferation by oxidative stress in normal prostate cells ---------- 51

Figure 2 Generation of *Nkx3.1; Gpx3* knockout mice and representative pictures of genitourinary tract and weighing results ---------- 53

Figure 3 The mRNA expression of prostate in *Nkx3.1; Gpx3* knockout mouse ---------- 56

Figure 4 ROS levels and antioxidant enzyme activity in *Nkx3.1; Gpx3* knockout mice ---------- 58

Figure 5 Histopathological Analysis of prostate in *Nkx3.1; Gpx3* KO mice ---- 60

LIST OF TABLES

LITERATURE REVIEW

TABLE I ROS modulating drugs undergoing clinical trials in oncology ---------- xxi

TABLE II Repurposed drugs currently in clinical trials for oncology - xxv

CHAPTER III

Table 1 Gene-specific primers ---------- 47

LIST OF ABBREVIATION

ROS	reactive oxygen species
FBS	fetal bovine serum
PS	penicillin/streptomycin
DMSO	dimethyl sulfoxide
MTT	thiazolyl blue tetrazolium bromide
PBS	phosphate buffered saline
PE	plating efficiency
SF	survival fraction
DCFH-DA	2’,7’-dichlorofluorescin diacetate
DCF	2’,7’-dichlorofluorescin
PCR	polymerase chain reaction
EMT	epithelial-mesenchymal transition
PSA	prostate-specific antigen
DPI	diphenylene iodonium
GSH	glutathione
NIH	National Institute of Health
GUT	genitourinary tract
SOD	superoxide dismutase
PIN	prostate intraepithelial neoplasia
EC50	half maximal effective concentrations
GPX3	Glutathione peroxidase 3
TRAMP	transgenic adenocarcinoma of the mouse prostate
NOS	nitric oxide synthase

GENERAL INTRODUCTION

Prostate cancer is the most diagnosed non-skin cancer in US men and is a leading cause of cancer-related death (1). In 2019, 174,650 people will be diagnosed with prostate cancer in the US and 31,620 are expected to die (2). Prostate cancer is age-related, and increasing reactive oxygen species (ROS) play an important role in the development and progression of prostate cancer (3). ROS assists cancer cell proliferation, invasion and metastasis and inhibits apoptosis leading cancer progression (4).

Phloretin (CAS number, 60-82-2) is a flavonoid found in Rosaceae (e.g., apples and pears) with known anti-inflammatory and immunosuppressive effects in lymphoid- and myeloid-derived cell lines (5). Moreover, phloretin exhibits anticancer activity via inducing apoptosis in human leukemia cells, bladder cancer, and colorectal cancer (6, 7), as well as inhibiting growth, invasion, and migration in human liver cells (8).

Pimozide is a United States Food and Drug Administration-approved antipsychotic, and is used to treat Tourette syndrome and schizophrenia (9). Pimozide has shown anticancer effects in leukemia (10), melanoma (11), retinoblastoma (12), breast cancer (13), prostate cancer (14), hepatocellular carcinoma (15), and osteosarcoma (16). The first reported anticancer effect of pimozide was that it acts as a dopamine antagonist in melanoma (17). It was also reported to inhibit STAT5 in leukemia (10), and to function as a STAT3 inhibitor in prostate cancer (14) and hepatocellular carcinoma (18). Recently, the ability of ROS generation to suppress osteosarcoma has been reported (16).

Oxidative stress contributes to cancer initiation, promotion, and progression (19). Under normal physiological conditions, cells have sufficient antioxidant capacity to eliminate ROS (20). However, increased ROS production or decreased antioxidant activity can lead to chronic oxidative stress. Glutathione peroxidase 3 (*GPX3*) plays an important role in ROS elimination. Silencing *GPX3* expression has been reported to enhance metastasis of human thyroid cancer cells and gastric cancer cells (21, 22). Inflammatory colorectal cancer was induced in *Gpx3* knockout mice, and it has been reported to increase inflammation, proliferation and DNA damage of colorectal cancer. In addition, the expression of genes associated with oxidative stress was altered, which means that *Gpx3* plays an important role in the development of tumors as a ROS scavenger (23).

ROS signaling by chronic oxidative stress is known to play an important role in the development of tumors and progression to malignancy (24). An antioxidant defense system in the body balances oxidative stress by removing ROS, which is called redox homeostasis (25). Depending on the degree of ROS, the effect of ROS on the tumor is different. When the concentration of ROS is low, ROS promotes cell proliferation and angiogenesis. When the concentration of ROS increases, ROS induces apoptosis by inducing lipid, protein, and DNA deformation. When the concentration of ROS is much higher, apoptosis is caused by DNA damage and cancer cells die.

In this study, I analyzed the roles and mechanism of anticancer agents, phloretin and pimozide and antioxidant enzyme *Gpx3* based on oxidative stress in prostate cancer *in vitro* and *in vivo*. In addition, the roles of redox homeostasis in the prostate cancer depending on the stages and levels of oxidative stress was confirmed by inducing oxidative stress in different models.

LITERATURE REVIEW

Prostate cancer and Oxidative stress

According to the International Agency for Research on Cancer, the incidence of prostate cancer among male cancer patients is highest in the United States (Fig. I) (2). In Korea, it is expected that the incidence of prostate cancer will increase due to the westernization of eating habits and the extension of the average life expectancy. Epidemiological, experimental, and clinical studies have shown evidence of increased exposure to oxidative stress in prostate cancer (3). Reactive oxygen species (ROS) signaling by chronic oxidative stress is known to play an important role in the development of tumors and progression to malignancy (24). Hydroxyl radicals, peroxides and superoxide are ROS that occur during normal cell metabolism every day. ROS may be inherently caused by mitochondria, metabolic processes, or inflammation, or may be due to external factors (26). ROS play an important role in regulating biological phenomena. ROS production has traditionally been interpreted as a pathological indicator such as infection, aging, mitochondrial DNA mutation, and cell proliferation. However, it is now noted that ROS production is associated with tumorigenesis and abnormal growth and proliferation of cells (27, 28). Proliferation, apoptosis, and senescence may be due to the activation of signaling pathways by intracellular ROS changes (29). Thus, excessive ROS production or lack of antioxidant defense systems may cause cells to experience oxidative stress, and increased ROS may play a wider role in the initiation and development of prostate cancer.

Estimated New Cases

	Males			Females	
Prostate	174,650	20%		Breast	268,600	30%
Lung & bronchus	116,440	13%		Lung & bronchus	111,710	13%
Colon & rectum	78,500	9%		Colon & rectum	67,100	8%
Urinary bladder	61,700	7%		Uterine corpus	61,880	7%
Melanoma of the skin	57,220	7%		Melanoma of the skin	39,260	4%
Kidney & renal pelvis	44,120	5%		Thyroid	37,810	4%
Non-Hodgkin lymphoma	41,090	5%		Non-Hodgkin lymphoma	33,110	4%
Oral cavity & pharynx	38,140	4%		Kidney & renal pelvis	29,700	3%
Leukemia	35,920	4%		Pancreas	26,830	3%
Pancreas	29,940	3%		Leukemia	25,860	3%
All Sites	**870,970**	**100%**		**All Sites**	**891,480**	**100%**

Estimated Deaths

	Males			Females	
Lung & bronchus	76,650	24%		Lung & bronchus	66,020	23%
Prostate	31,620	10%		Breast	41,760	15%
Colon & rectum	27,640	9%		Colon & rectum	23,380	8%
Pancreas	23,800	7%		Pancreas	21,950	8%
Liver & intrahepatic bile duct	21,600	7%		Ovary	13,980	5%
Leukemia	13,150	4%		Uterine corpus	12,160	4%
Esophagus	13,020	4%		Liver & intrahepatic bile duct	10,180	4%
Urinary bladder	12,870	4%		Leukemia	9,690	3%
Non-Hodgkin lymphoma	11,510	4%		Non-Hodgkin lymphoma	8,460	3%
Brain & other nervous system	9,910	3%		Brain & other nervous system	7,850	3%
All Sites	**321,670**	**100%**		**All Sites**	**285,210**	**100%**

Fig. I Prostate cancer is the most commonly diagnosed cancer in men (2). Ten Leading Cancer Types for the Estimated New Cancer Cases and Deaths by Sex, United States, 2019.

Redox homeostasis

An antioxidant defense system in the body balances oxidative stress by removing ROS, which is called redox homeostasis (25). ROS are formed by mitochondrial respiration and enzymatic catalysis including NADPH oxidase (NOX), xanthine oxidase, nitric oxide synthase (NOS), arachidonic acid, and metabolizing enzymes such as the cytochrome P450 enzymes, lipoxygenase, and cyclooxygenase (30). Different types of antioxidants play an important role in redox homeostasis, including dietary natural antioxidants (e.g., vitamins A, C, and E), endogenous antioxidant enzymes (e.g., superoxide dismutase, catalase, glutathione peroxidase, glutathione reductase, and peroxiredoxins), and antioxidant molecules (e.g., glutathione, coenzyme Q, ferritin, and bilirubin) (31). When redox homeostasis collapses due to long-term oxidative stress, ROS induces mutations in the DNA of cells and induces tumorigenesis (32). Oxidative stress plays an important role in various stages of tumorigenesis. ROS is produced by several intrinsic or extrinsic stimuli. ROS damages the DNA**,** lipids, and proteins of the cell and causes a deadly effect on the cell (33). However, depending on the degree of ROS, the effect of ROS on the tumor is different. When the concentration of ROS is low, ROS promotes cell proliferation and angiogenesis. When the concentration of ROS increases, ROS induces apoptosis by inducing lipid, protein, and DNA deformation. When the concentration of ROS is much higher, apoptosis is caused by DNA damage and cancer cells die. It has been reported that the removal of ROS by the antioxidant system helps to the development, survival, and drug resistance of cancer cells (Fig. II) (4).

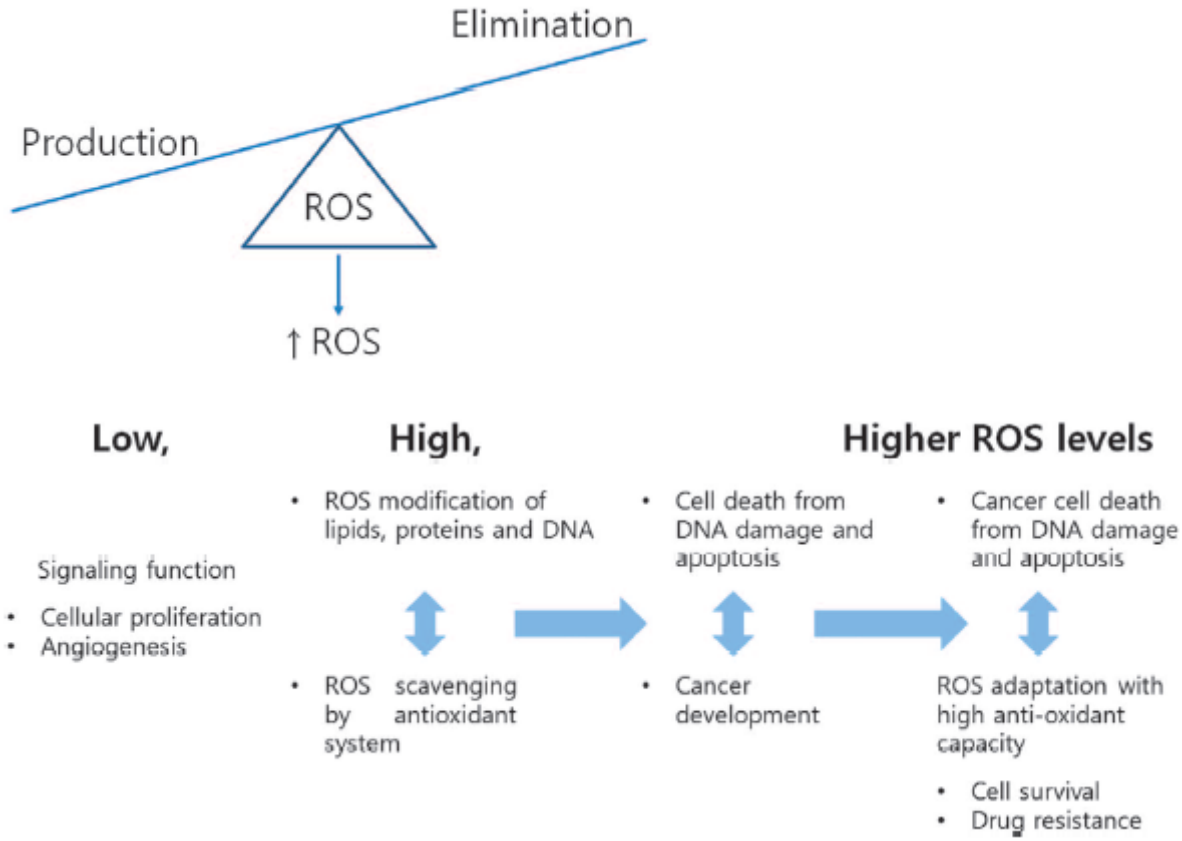

Fig. II Roles of ROS in cancer according to ROS level (4). Low levels of ROS can activate various signaling pathways to stimulate cell proliferation and survival. Adaptation to persistent and high levels of ROS can promote cancer development, survival of cancer cells and resistance to chemotherapeutics.

Cellular response to ROS is difficult to predict

ROS mediates motility, invasiveness, extracellular matrix remodeling, neo-angiogenesis, and metabolic reprogramming of cancer cells (34). ROS activates or inhibits telomerase activity, contributing to metabolic reprogramming, invasion, and metastasis of cancer cells (35). To remove ROS, cancer cells express the ROS scavenging enzyme (36). Accumulating ROS in hypoxic cancer cells increases SOD expression, converting superoxide to less reactive hydrogen peroxide. Hydrogen peroxide is broken down into water and dioxygen by antioxidant enzymes or antioxidants. The balance between production and degradation of ROS leads to redox homeostasis.

ROS is reported to be both cytotoxic and tumorigenic (35). Low levels of ROS activate mechanisms involved in cell proliferation and survival (37). The anti-ROS strategy is expected to inhibit tumorigenesis by inhibiting the oncogenic function of ROS (36). However, increasing the expression of Nuclear Respiratory Factor 2, which increases the expression of antioxidant genes, or treating antioxidants may not only reduce ROS levels of cancer cells but also increase oncogenic activity (38). The ability of mitochondria and the detoxification of ROS are known to be important for the survival of cancer cells, since excessive levels of ROS damage cell macromolecular components, leading to cell death (34). Because cancer cells are more vulnerable than normal cells to disrupting redox balance and mitochondrial function, the main principal of chemotherapy is thought to break down the redox homeostasis of cancer cells (39). However, the assumption that cancer cells already have high ROS levels and inhibit ROS removal ability to kill cancer cells with ROS toxicity is oversimplification (4). Cancer cells express high antioxidant systems in order to survive in a high oxidative stress environment (40), which acts as a resistance mechanism of anticancer drugs.

Recent reports suggest that the benefits of modulating ROS are difficult to predict because the regulation of cellular signals to redox homeostasis is very complex and can vary depending on the cancer cell environment (41). The results on the therapeutic effect of ROS at the bedside are disappointingly inconsistent, and neither raising or lowering ROS shows a consistent therapeutic effect (42).

Controversy about chemotherapy with antioxidant

According to Sebastian et al., patients with advanced cancer had longer survival after receiving high-dose intravenous vitamin C therapy (43). Studies by Greenlee et al. have shown that recurrence of breast cancer is reduced when Vitamin C is used, and that the risk of recurrence and mortality of breast cancer is reduced when Vitamin E is used (44). However, the use of antioxidants, selenium and vitamin E, to prevent prostate cancer has been reported to increase the risk of prostate cancer (42). Some anticancer drugs produce high levels of ROS, causing DNA damage and apoptosis, and can increase the effects by removing GSH from cancer cells. Drugs that cause cell death by altering redox homeostasis in the cell are being studied to improve existing drugs. Based on these studies, anti-cancer agents that inhibit the antioxidant enzyme glutathione have been developed (Table I) (31).

Table I. ROS modulating drugs undergoing clinical trials in oncology (31).

Drug	Mechanisms of action	Cancer type	Outcome
L-Buthionine-sulfoximine	Inhibits GSH synthesis; activates PKCδ	Neuroblastoma Melanoma	Efficacious *in vitro*
Menadione	Depletes GSH; activates ERK1/2 and p38MAPK	Gastrointestinal and lung cancer	Under clinical trial
Imexon	Depletes intracellular thiols; increases AP-1 and Nrf2-DNA binding activity	advanced breast cancer; NSCLC; prostate and pancreatic tumors	Efficacious
Disulfiram	Oxidizes GSH and inhibits proteasome; activates JNK; inhibits Nrf2 and NF-κB	Metastatic melanoma; liver cancer	Under clinical trial
Bortezomib	Inhibits proteasome activity; activates NF-κB; activates Nrf2 and upregulates HO-1	Myeloma, leukemia, AML, myelodysplastic syndrome, neuroblastoma, prostate cancer	Under clinical trial
NOV-002	Oxidizes GSH and induces S-glutathionylation	NSCLC; breast and ovarian cancer	Efficacious
Ezatiostat	Inhibits GST-P1 and activates JNK/ERK	Myelodysplastic syndrome	Under clinical trial
PX-12	Inactivates Trx-1	Advanced solid tumors	Efficacious
Dimesna	Targets Trx and Grx	Ovarian carcinoma, NSCLC	Efficacious
Metexafin gadolinium	Inhibits Trx	pancreatic, biliary and haematological cancer, renal carcinoma	Under clinical trial
Arsenic troxide	Oxidizes GSH and thiol enzymes	APL, melanoma	Efficacious

Phloretin

Phloretin (3-(4-hydroxyphenyl)-1-(2,4,6-trihydroxyphenyl) propan-1-one) is a dihydrochalcone with a C6–C3–C6 backbone (45). Phloretin is obtained from apples and apple-derived substances and conjugates with glucosidic to form phloridzin (phloretin 2′-O-glucose) (46). Glycosylated derivatives are converted to the free form by hydrolytic enzymes in the small intestine (46). Phloretin glycosides are present at high levels in commercially available apple purees and juices as a result of the manufacturing process (47). Phloretin has a variety of biological activities, including anti-oxidative and ant-cancer effects, and prevents cardiovascular diseases (48, 49). It also inhibits the production of inflammatory chemokines, cytokines and differentiation factors induced by leukocytes activated by an innate immune response (50). Phloretin induces apoptosis in human leukemia cells, bladder cancer, and human colon cancer cells (6-8). Phloretin inhibited growth, invasiveness and migration in human liver cancer cells (51). Phloretin is a selective inhibitor of GLUT2 and has a significant anticancer effect by inhibiting trans-membrane glucose transport (51-53). Phloretin also induced cell cycle arrest and apoptosis by ROS production and activating mitochondrial apoptotic pathway in glioblastoma cells (54).

Pimozide as drug repurposing for cancer

New advances in drug discovery and development are needed to make drug pharmaceutical research more predictable and reliable (55). One of the most important approaches is drug repurposing. Drug repurposing is a way of looking for new applications of already existing or abandoned drugs (56, 57). In cancer therapy, these methods are finding significant results by finding new uses for existing drugs (Table II)

(58, 59). For example, metformin is a widely used antidiabetic drug. However, metformin functions as an anticancer agent by inhibiting the growth of cancer cells *in vitro* and *in vivo* (60). Disulfiram is a drug for alcoholism, but suppresses the self-renewal of glioblastoma (61). In addition, imatinib (Gleevec) was developed to treat chronic myleogeneous leukemia, but has been used to treat gastrointestinal stromal tumors (62) and colorectal cancer (63) with similar mechanisms. Pimozide is an FDA-approved neuroleptic drug and belongs to the diphenylpiperidine class of drugs. It is mainly used to treat Tourette syndrome and schizophrenia (9). Pimozide has anticancer effects on melanoma (17), breast cancer (13) and myelogenous leukemia (64). Pimozide inhibited the self-renewal ability of chronic myelogenous leukemia by inhibiting STAT5 activity (64). In addition, inhibition of STAT3 inhibited the maintenance and tumorigenicity of hepatocellular carcinoma stem-like cells (18). Recently, the ability of ROS generation to suppress osteosarcoma has been reported (16).

GPX3

Glutathione peroxidase (GPX) is present in various tissues (65-67), and plays an important role in ROS elimination. Four types exist: cellular GPX1, gastrointestinal GPX2, extracellular GPX3, and phospholipid hydroperoxide GPX4, which are antigenically, structurally, and enzymatically different (68). GPX3 plays an important role in ROS elimination. Silencing *GPX3* expression has been reported to enhance metastasis of human thyroid cancer cells and gastric cancer cells (21, 22). Inflammatory colorectal cancer was induced in *Gpx3* knockout mice, and it has been reported to increase inflammation, proliferation and DNA damage of colorectal cancer. In addition, the expression of genes associated with oxidative stress was altered,

which means that *Gpx3* plays an important role in the development of tumors as a ROS scavenger (23). Several studies have reported that *Gpx3* is associated with Wnt/β-catenin signaling (21, 23) or p53-induced gene 3 signaling (69). Also, *Gpx3* can arrests the cell cycle in lung cancer cell lines through ROS-MKP3-Erk-NF-κB-Cyclin B1 pathway (70).

Table II. Repurposed drugs currently in clinical trials for oncology (59).

Drug	Trade name	Original indication	Number of clinical trial
Acetylsalisylic acid	Aspirin	Pain, fever, inflammation	31
Artesunate	Artesunate, ansunate, artex, plasmotrim	Malaria	3
Auranofin	Ridaura	Rheumatoid arthritis	2
Digoxin	Lanoxin	Heart conditions	4
Disulfiram	Antabuse	Alcoholism	5
Doxycycline	Doxycylin, doxylin, doxyhexal	Bacterial infections	7
Itraconazole	Sporanox	Fungal infections	14
Leflunomide	Arava, arabloc, lunava, repso, elafra	Rheumatism	1
Lithium	Lithium Carbonate ER, lithobid, eskalith	Depression	3
Mebendazole	Vermox	Worm infections	3
Metformin	Glucophage	Diabetes II	94
Naproxen	Aleve, Naprosyn	NSAID, anti-inflammatory	2
Nelfinavir	Viracept	HIV infection	7
Ritonavir	Norvir	HIV infection	6
Statins		High cholesterol	37
Thalidomide	Immunoprin	Sedative, anti-nausea	195

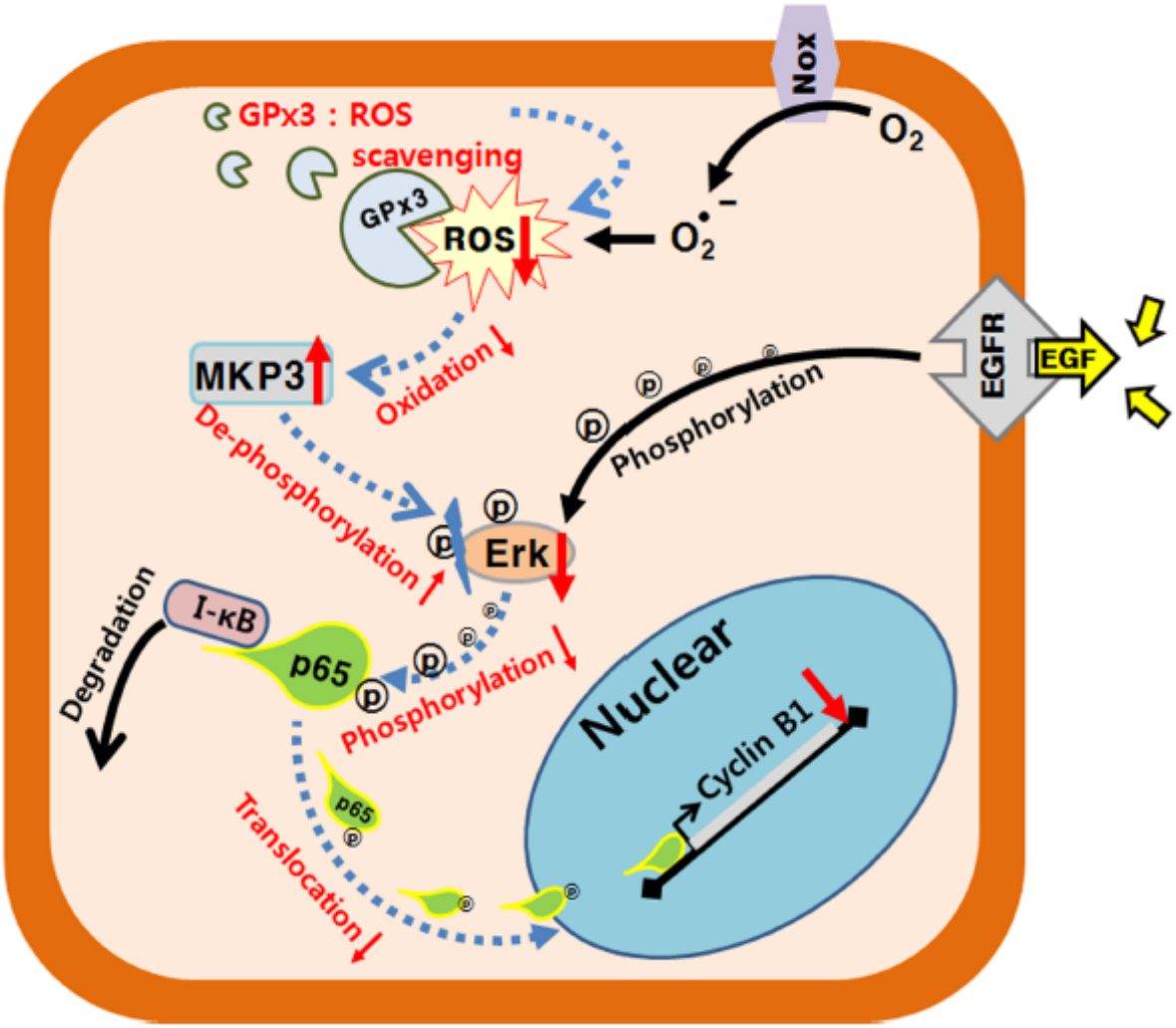

Fig. III Antioxidant *GPX3* could mediate lung cancer suppression (70). *GPX3* can arrests the cell cycle in lung cancer cell lines through ROS-MKP3-Erk-NF-κB-Cyclin B1 pathway

CHAPTER I

Phloretin inhibits the human prostate cancer cells through the generation of reactive oxygen species

1 INTRODUCTION

According to annual reports (1975–2011) from the United States government, prostate cancer occurs in men at significantly higher rates than other cancers (71). Globally, prostate cancer is the second most common tumor and the sixth leading cause of death among men (72). The strong association between this cancer and age is due to the large role of signaling pathways involving reactive oxygen species (ROS) in cancer development and progression (3). In general, ROS influences cancer development through promoting cell proliferation, invasion, and metastasis while inhibiting apoptosis. However, ROS also has anti-cancer effects, including inducing cell cycle arrest, apoptosis, and necrosis (40).

Oxidative stress also regulates β-catenin action (73). This effector protein interacts with TCF/LEF-1 to activate Wnt target genes during Wnt/β-catenin signaling, a pathway that is associated with both normal prostate development and prostate cancer progression (74). During this signaling process, β-catenin degradation is inhibited, leading to intracellular or nuclear accumulation (75). Specifically, prostate cancer progression is linked to nuclear β-catenin accumulation (76). Research using HEK293 (human embryonic kidney) cells revealed that H2O2-induced oxidative stress suppressed Wnt/β-catenin signaling, whereas the activation of this pathway inhibited H2O2-induced apoptosis (77).

Phloretin (CAS number, 60-82-2) is a flavonoid found in Rosaceae (e.g., apples and pears) with known anti-inflammatory and immunosuppressive effects in lymphoid- and myeloid-derived cell lines (5). Moreover, phloretin exhibits anticancer activity via inducing apoptosis in human leukemia cells, bladder cancer, and colorectal cancer (6, 7), as well as inhibiting growth, invasion, and migration in human liver cells

(8). However, we do not know what role, if any, ROS generation plays in phloretin antitumor function. In this study, we demonstrated how phloretin affects prostate cancer cells and described associated molecular mechanisms. Our work is the first to provide empirical evidence that phloretin inhibits prostate cancer through generating ROS and downregulating Wnt/β-catenin signaling.

2 MATERIALS AND METHODS

2.1 Reagents

Human prostate cancer cell lines PC-3 and DU145, and African green monkey kidney-derived Vero cell were acquired from the American Type Culture Collection (Manassas, VA, USA). PC-3 and DU145 cells were cultured in RPMI 1640 medium (Welgene, Gyeongsan, South Korea) supplemented with 10% fetal bovine serum (FBS) (Gibco, Grand Island, NY, USA) and 1% penicillin/streptomycin (PS) (Gibco) at 37℃ in 95% air/5% CO2. Vero cell was cultured in DMEM medium (Welgene) supplemented with 10% FBS and 1% PS at 37℃ in 95% air/5% CO2. Phloretin (Sigma, St. Louis, MO, USA) was dissolved in dimethyl sulfoxide (DMSO) (Duksan Pure Chemical Co., Ansan, South Korea) to obtain concentration of 100 mM. The final DMSO concentration in the solution was 0.1%. DMSO at the same final concentration of 0.1% was used as control.

2.2 Cell proliferation assay

The proliferation capacity of cells was analyzed using thiazolyl blue tetrazolium bromide (MTT) (Sigma) assay based on the ability of live cells to convert tetrazolium salt into purple formazan. Briefly, PC-3, DU145, and Vero cells were seeded into 96-well cell culture plates (SPL Life Science, Pocheon, South Korea) at a density of 1.6 x 104 per well in 200 ㎕ media. After 24 h of culturing, the medium was replaced to FBS free media for 24 h. Cells were treated with phloretin at concentration of 20, 50, 100 μM or vehicle (DMSO) control and cultured for 24 h. The medium was then

changed with 100 ㎕ of MTT (diluted to 1 mg/ml in FBS-free medium from a stock solution of 5 mg/ml) and incubated at 37℃ for 3 h. The supernatant was eliminated and 100 ㎕ of DMSO was supplemented to each well to dissolve the formazan crystals. Plates were agitated at room temperature for 5 min. The absorbance was read at 570 nm on an Epoch BioTek microplate reader (BioTek, Winooski, VT, USA). All treatments were performed in triplicates.

2.3 Clonogenic assay

To determine the long-term effects, Clonogenic assay using logarithmically-growing PC-3 and DU145 cells was performed. In brief, approximately 1000 cells obtained from sub-confluent cell culture flask (SPL) were seeded per 60 mm cell culture dishes (SPL) in 5 ml of medium. 24 h after seeding the cells, phloretin at concentrations of 20, 50, 100 μM or vehicle (DMSO) was added to the medium. The cells were allowed to form colonies for 7 days and were rinsed with fresh medium every 3 days. When the colonies were discrete and well defined, the dishes were washed with phosphate buffered saline (PBS) (Gibco) solution, fixed with methanol (Merck, Darmstadt, Germany), stained with hematoxylin (Yeong-Dong Diagnostics, Yongin, South Korea). The colonies per dish were counted using inverted microscope (Olympus IX70). Colonies with 50 cells or more were counted. Plating efficiency (PE) is the ratio of the number of colonies to the number of cells seeded. The number of colonies that arise after treatment of cells, expressed in terms of PE, is called the surviving fraction (SF).

2.4 Cell migration assay

Cell motility was analyzed using an in vitro wound healing assay. PC-3 and DU145 cells were seeded into 6-well cell culture plate (SPL) and grown to 90% or above confluence. Monolayers of prostate cells were then wounded using a pipette tip. Cell repair was monitored using an inverted microscope (Olympus IX70, Tokyo, Japan) following 24 h exposure to phloretin at concentrations of 20, 50, 100 μM or vehicle (DMSO). All treatments were performed in triplicates. The wounded areas were measured using Image J software (https://imagej.nih.gov/ij/).

2.5 ROS measurement

The generation of intracellular ROS was determined using 2',7'-dichlorofluorescin diacetate (DCFH-DA (Sigma) which is converted to fluorescent 2',7'-dichlorofluorescin (DCF) in the presence of peroxides. After exposure to different concentrations of phloretin for 24 h, PC-3 and DU145 cells were treated with 10 μM DCFH-DA for 1 h at 37℃ and washed with PBS. The cells were detached with trypsin-EDTA (Gibco), and intracellular ROS was detected using a fluorescence spectrometer Victor 3 (Perkin Elmer, Waltham, MA, USA) at 485 nm exposure and 535 nm emission

2.6 Real-time reverse transcription-polymerase chain reaction (PCR)

Total RNA was extracted using a Hybrid-R RNA extraction kit (GeneAll Biotechnology, Seoul, South Korea). cDNA was synthesized by M-MLV cDNA Synthesis kit (Enzynomics, Daejeon, South Korea) according to the supplier's

instructions. Quantitative real-time PCR was performed using TOPrealTM qPCR 2X PreMIX (Enzynomics) on a CFX Connect Real-Time PCR Detection system (Bio-Rad Laboratories, Hercules, CA, USA). Primers used were 5'-GGAAGCCATCAAACGTGACT-3' (sense) and 5'-CTGATTTGGACAAGCAGCAA-3' (antisense) for human SOD2 (NCBI gene ID: 6648); 5'-ACAGCAAACCGCACGCTATG-3' (sense) and 5'-CAGTGGTCAGGACATCAGCTTTC-3' (antisense) for human Catalase (NCBI gene ID: 847); 5'-CGCTTCCAGACCATTGACATC-3' (sense) and 5'-CGAGGTGGTATTTTCTGTAAGATCA-3' (antisense) for human Gpx1 (NCBI gene ID: 2876); 5'-ACATGCCTACAGGTATGCGT-3' (sense) and 5'-GAGCAGAACAATTGGACCTA-3' (antisense) for human Gpx3 (NCBI gene ID: 2878); 5'-TTGGCTACCTTGCAGTTCGT-3' (sense) and 5'-ATGTGAACCATCGCAGGCA-3' (antisense) for human CISD2 (NCBI gene ID: 493856); 5'-CTCGGACAAGCTGAGCAAGA-3' (sense) and 5'-GCTCTGGAGGACCTGGTAGA-3' (antisense) for human Twist1 (NCBI gene ID: 7291); 5'-ATGACTCGAGCTCAGAGGGT-3' (sense) and 5'-ATTGCACGTGTGGCAAGTTC-3' (antisense) for human β-catenin (NCBI gene ID: 399274); 5'-CCTGGCACCGTAGGACAAAT-3' (sense) and 5'-TGGGACCATATGGGGAGGG-3' (antisense) for human TCF4 (NCBI gene ID: 6934); 5'-GTGAAGATGGAAGGGCACGA-3' (sense) and 5'-CATGTTGCTCACGGAGGAGT-3' (antisense) for human FoxA2 (NCBI gene ID: 3170); 5'-CATGTACGTTGCTATCCAGGC-3' (sense) and 5'-CTCCTTAATGTCACGCACGAT-3' (antisense) for human β-actin (NCBI gene ID: 60). Ratio of target gene fold-change was normalized to human β-actin expression using comparative CT (2-ΔΔCt) method.

2.7 Statistical analysis

All data are presented as mean ± standard error. Statistical significance ($P < 0.05$) was further analyzed with Student's t-test using computer program GraphPad Prism 5 (GraphPad Software, La Jolla, CA, USA)

3 RESULTS

3.1 Phloretin inhibits cell proliferation and colony formation in the PC3 and DU145 cell lines

We first analyzed the effect of phloretin on cell proliferation and colony formation. In the PC3 and DU145 prostate cancer cell lines, cell growth was inhibited by phloretin at various concentrations for 24 h (Fig. 1). As a negative control for prostate cancer, phloretin was treated in Vero cells derived from African green monkey and as shown in Fig. 1, it did not affect the proliferation of Vero cells. Phloretin also inhibited colony formation in two prostate cancer cell lines (Fig. 2a) and we counted the number of surviving colonies (Fig. 2b).

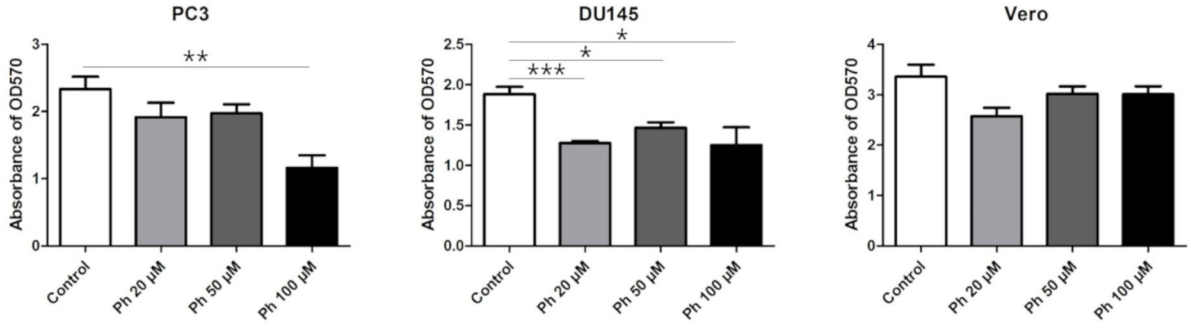

Fig. 1 The effect of phloretin on cell proliferation. The inhibition of proliferation of PC3 and DU145 by phloretin was confirmed by MTT assay. But, phloretin has no effect of normal cell line Vero cells derived from normal African green monkeys. Results are presented as means ± SEM.

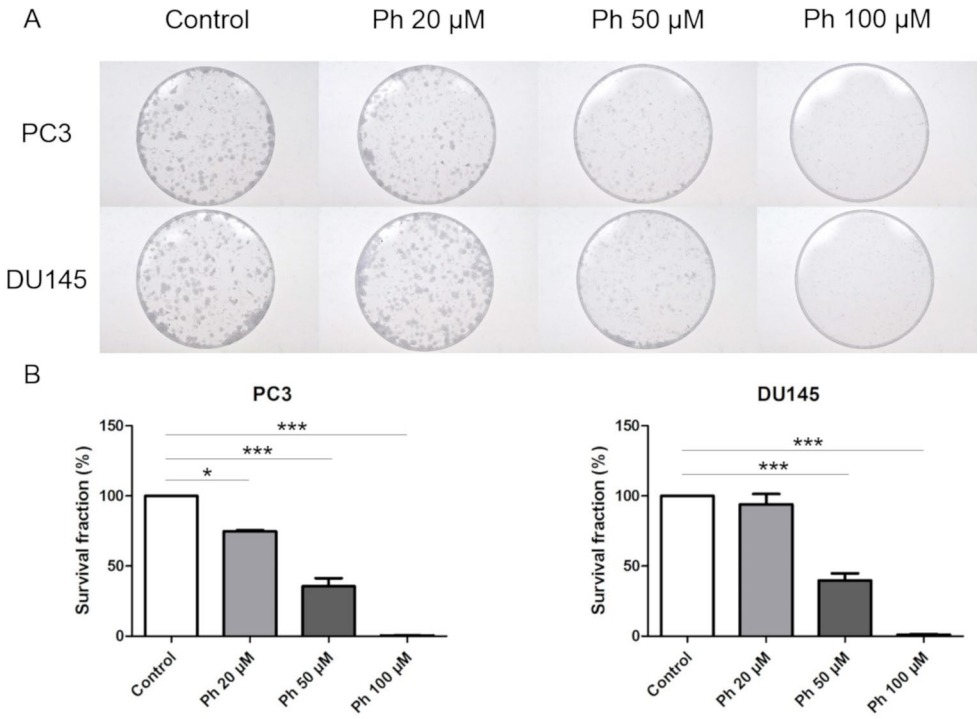

Fig. 2 The effect of phloretin on colony formation. To determine long term effect of phloretin, PC3 and DU145 cells were allowed to form colonies for 7 days. Colony formation of prostate cancer cell lines was inhibited in a concentration-dependent manner. Results are presented as means ± SEM.

3.2 Phloretin inhibits migration of PC3 and DU145 cell lines

We evaluated the migration of cells by in vitro wound healing assay by treating phloretin with PC3 and DU145 cells. After 24 hours of incubation at various concentrations of phloretin, the migration of prostate cancer cells to the denuded area was inhibited in a dose-dependent manner (Fig. 3A). The area where the wound was recovered was quantitatively analyzed (Fig. 3B).

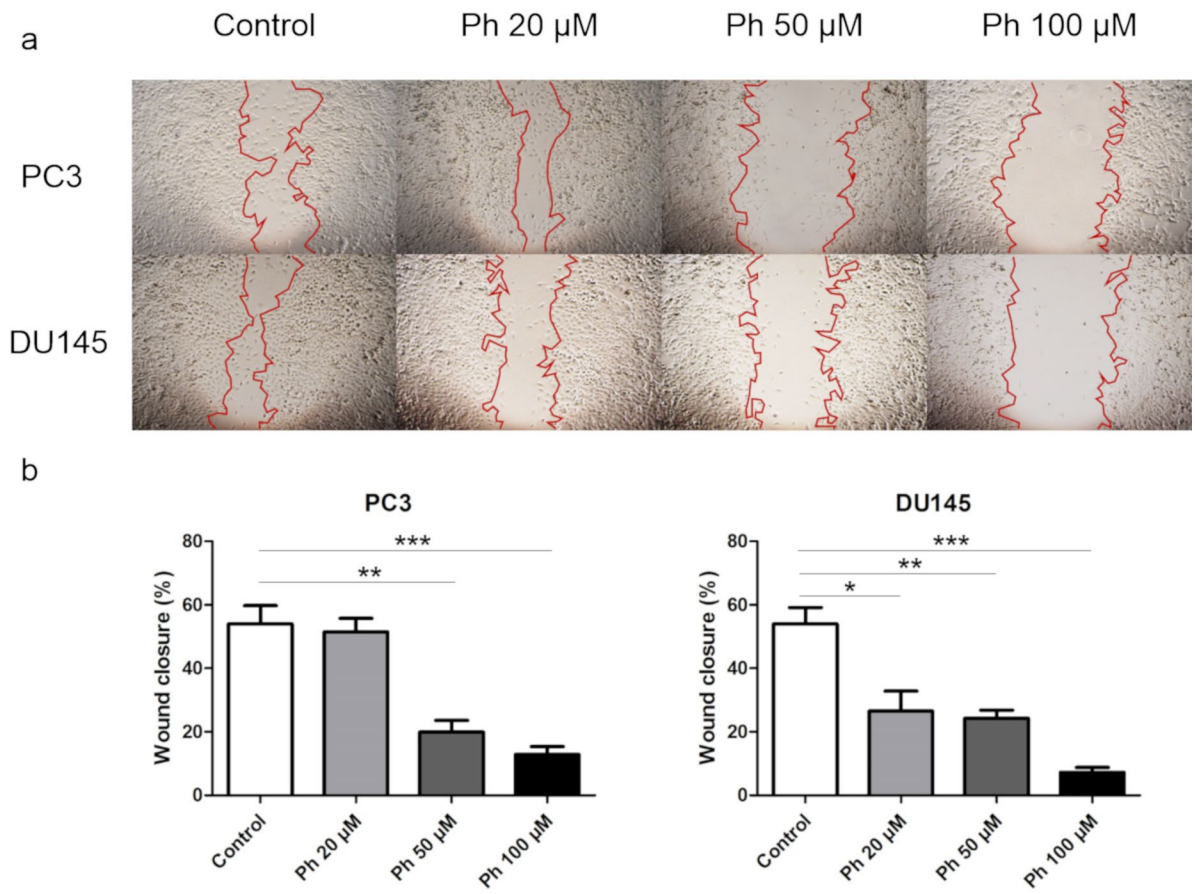

Fig. 3 The effect of phloretin on migration of PC3 and DU145. Phloretin suppressed the migration of PC3 and DU145 human prostate cancer cells. Cells that migrated to the wounded region were photographed (magnification, x40). Results are presented as means ± SEM.

3.3 Phloretin induces ROS accumulation in PC3 and DU145 cell lines through inhibiting antioxidant enzyme gene expression

According to reports, ROS accumulation is known to partially affect the proliferation of cells. We treated PC3 and DU145 cells with various concentrations of phloretin and measured the amount of ROS present in the cells using DCFH-DA, a fluorescent dye, after 24 hours. As expected, ROS levels increased after treatment with phloretin in PC3 and DU145 (Fig. 4). In addition, gene expression of SOD2, Catalase, Gpx1, Gpx3 and CISD2 genes related to ROS production was analyzed. Phloretin treatment resulted in decreased expression of SOD2, Catalase, Gpx1 and CISD2 in PC3 and DU145 (Fig. 5). However, Gpx3 expression increased at a medium concentration of 50 μM and decreased at a high concentration of 100 μM. Presumably, the production of ROS by phloretin seems to be related to the expression of antioxidant enzyme genes.

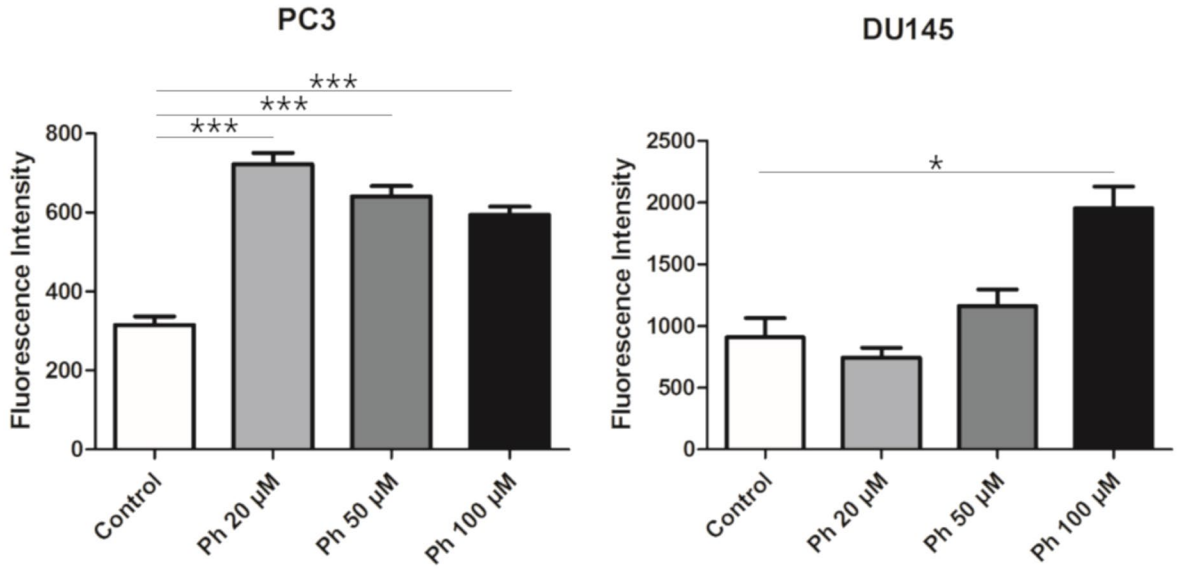

Fig. 4 Phloretin induced generation of ROS in the PC3 and DU145 cell lines. Fluorescence spectrometer was used to determine ROS generation after staining with DCFH-DA. Results are presented as means ± SEM.

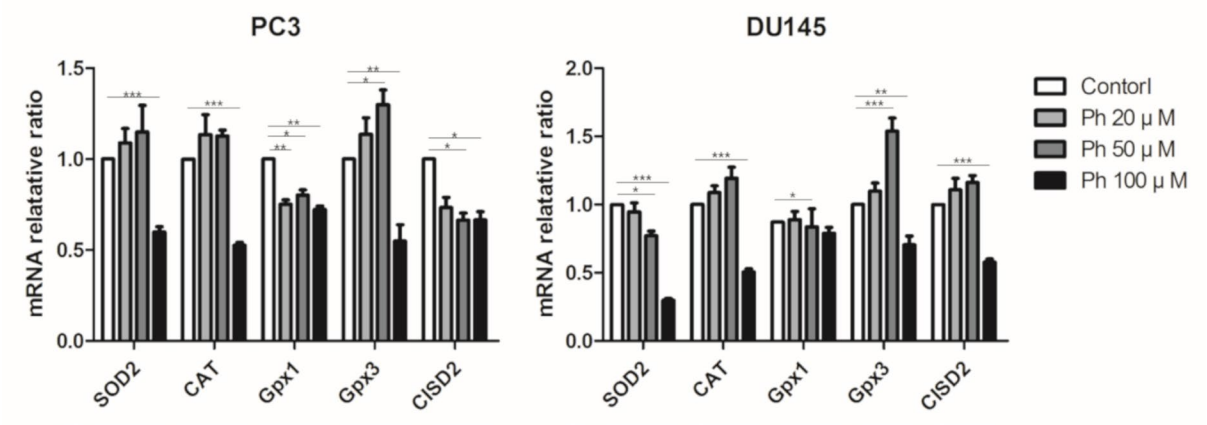

Fig. 5 The effect of phloretin on mRNA expression levels of SOD2, CAT, Gpx1, Gpx3 and CISD2 in PC3 and DU145 cells. Phloretin downregulated the mRNA expression levels of anti-oxidant enzymes in PC3 and DU145 cells. The mRNA expression levels of CISD2 was downregulated in PC3 and DU145 cell. Results are presented as means ± SEM.

3.4 Phloretin downregulates the mRNA levels of Wnt/β-catenin signaling in PC3 and DU145 cell lines

When the Wnt/β-catenin pathway is activated, β-catenin enters the nucleus and increases the expression of the target gene in the down-stream. We therefore analyzed the expression of β-catenin, TCF4, FoxA2, and c-Myc when phloretin was treated with PC3 and DU145 cells (Fig. 6). The expression of β-catenin, TCF4, and FoxA2 decreased in PC3 and DU145 after treatment with phloretin. However, c-Myc decreased in PC3 but increased in DU145. Wnt/β-catenin signaling has been reported to be associated with the epithelial-mesenchymal transition (EMT) of prostate cancer (78). The expression of Twist associated with EMT was analyzed and the expression was decreased in both PC3 and DU145.

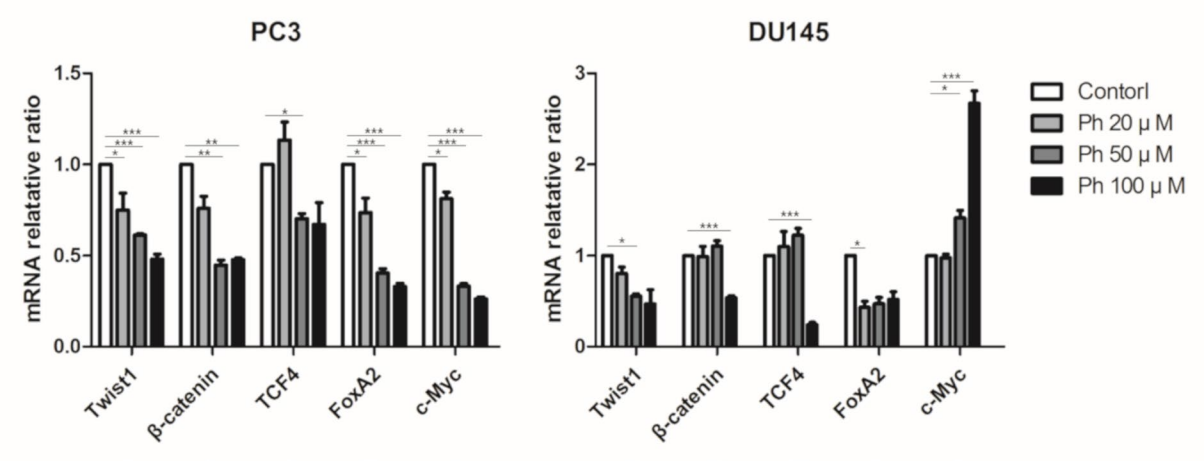

Fig. 6 The effect of phloretin on mRNA expression levels of Twist1, β-catenin, TCF4, FoxA2, and c-Myc in PC3 and DU145 cells. The mRNA expression levels of Twist1, β-catenin, TCF4 and FoxA2 in PC3 and DU145 cells were downregulated. However, c-Myc decreased in PC3 but increased in DU145. Results are presented as means ± SEM.

4 DISCUSSION

First, we confirmed that phloretin inhibited the proliferation of prostate cancer cell lines PC3 and DU145. To verify whether this effect is specific to cancer cells, we then followed procedures in previous reports (79, 80), to repeat phloretin treatment in Vero cells, a normal line derived from African green monkeys. Phloretin did not affect Vero cell proliferation, indicating specificity to prostate cancer cells. Our findings corroborate earlier reports of phloretin inhibiting human glioblastoma cell proliferation (54).

Furthermore, we confirmed that the anticancer effect of phloretin is related to ROS production, as previously described (54). Overall, medical trials have not found a significant relation between prostate cancer incidence and the intake of antioxidant supplements such as Vitamin C (81). However, this lack of a connection may be because ROS anticancer effects depend on tumor stage (4). For instance, antioxidants significantly reduced prostate cancer in patients with normal prostate-specific antigen (PSA), a biomarker of prostate cancer risk, whereas antioxidants significantly increased prostate cancer in patients with above-baseline PSA levels (81). Previously, we used a Gpx3-knockout TRAMP mouse model (highly susceptible to tumors) to show that a decrease in Gpx3 expression is associated with prostate cancer development (82). The downregulation of Gpx3 dampened ROS removal processes, thus elevating oxidative stress in TRAMP mice, and such an outcome during the pre-neoplastic stage likely contributed to cancer development. Together, these data suggest that antioxidants and ROS signaling may exert different effects depending on the stage of prostate cancer.

The redox-sensitive protein CISD2 belongs to the CDGH iron sulfur domain-containing family (83) and is found in mitochondria (84) and ER (85), both major ROS sources. In lung cancer cells, CISD2 depletion corresponds to an increase in ROS production (86). Likewise in prostate cancer cells, CISD2 probably acts to maintain redox homeostasis through removing ROS. This elevated antioxidant ability in cancer cells increase drug resistance and ensure their survival (4). We found that phloretin treatment led to ROS production in prostate cancer cells, suggesting that ROS concentrations may have exceeded the functional capacity of antioxidant enzymes. Corroborating this hypothesis, CISD2 expression was downregulated, in conjunction with the expression of antioxidant enzymes SOD2, catalase, Gpx1, and Gpx3. However, treatment with 20 μM and 50 μM phloretin increased Gpx3 expression, possibly to compensate for lower SOD2, catalase, and Gpx1 levels. Indeed, previous research on Nkx3.1 knockout mice also found evidence of this compensatory mechanism; elevated Qscn6 expression caused oxidative stress, but while Gpx2 and Prdx6 decreased, Gpx3 expression increased (87).

Our analysis of Wnt/β-catenin signaling confirmed its importance in prostate cancer (76). In both cancer cell lines (DU145 and PC3), phloretin decreased the expression of β-catenin and two targets, TCF4 and FoxA2. However, c-Myc expression decreased in PC3 and increased in DU145. This β-catenin target is associated with apoptosis (88). We observed that c-Myc inhibition suppressed apoptosis in DU145 (though no change was detected in PC3). Furthermore, when DU145 cells were treated with the anticancer agent Paclitaxel, c-Myc expression increased in conjunction with apoptosis (89). Overexpression of c-Myc caused an increase in colcemid-induced apoptosis was increased (90). Taken together, these results suggest that c-Myc overexpression is associated with apoptosis in DU145, but

not in PC3. Furthermore, phloretin reduced the expression of Twist1. Twist1 is associated with the epithelial mesenchymal transition and invasion of prostate cancer (91). Further studies are needed to determine whether Phloretin inhibits prostate cancer invasion and metastasis.

Collectively, the results of this study suggest that phloretin has a therapeutic effect on prostate cancer in vitro, inhibiting the proliferation and migration of cancer cell lines PC3 and DU145. The mechanism of phloretin appears to be increasing ROS production. In addition, phloretin reduced the expression of SOD2, catalase, Gpx1, and Gpx3, along with their regulator CISD2. Phloretin also inhibited Wnt/β-catenin signaling in PC3 and DU145, while reducing Twist1 expression. We thus recommend phloretin as a promising anticancer therapeutic agent.

Chapter II

Pimozide Inhibits the Human Prostate Cancer Cells through the Generation of Reactive Oxygen Species

1 INTRODUCTION

New strategies in drug discovery are needed for more reliable drug development (55). Among these strategies, drug repurposing is important to identify new applications of drugs that are already approved or abandoned (56, 57). Drug repurposing in cancer treatment has successfully identified new uses of existing drugs and achieved significant results (58). For example, metformin, a diabetic drug, has been reported to have anticancer activity in prostate cancer and several clinical trials are underway (92). Disulfiram, a drug for alcoholism, has also been reported to inhibit prostate cancer cell growth (93). Imatinib, developed to treat chronic myelogenous leukemia, is used to treat gastrointestinal stromal tumors (62) and colorectal cancer (63), which share a similar target.

Prostate cancer is the most commonly diagnosed non-skin cancer in men in developed countries and is a major cause of cancer-related deaths (1). In 2019, 174,650 men in the United States are expected to be diagnosed with prostate cancer and 31,620 will die from the diseases (2). Prostate cancer is closely related to age, and several signaling pathways involving reactive oxygen species (ROS), which increase with age, play important roles in the development and progression of cancer (3). In general, ROS promote cell proliferation, invasion, and metastasis, while inhibiting apoptosis, leading to cancer progression. Therefore, anticancer agents have been reported based on antioxidant effects (94). However, higher levels of ROS have anti-cancer effects, by causing cell cycle arrest, apoptosis, and necrosis (40).

Pimozide is a United States Food and Drug Administration-approved antipsychotic, and is used to treat Tourette syndrome and schizophrenia (9). Pimozide has shown anticancer effects in leukemia (10), melanoma (11), retinoblastoma (12),

breast cancer (13), prostate cancer (14), hepatocellular carcinoma (15), and osteosarcoma (16). The first reported anticancer effect of pimozide was that it acts as a dopamine antagonist in melanoma (17). It was also reported to inhibit STAT5 in leukemia (10), and to function as a STAT3 inhibitor in prostate cancer (14) and hepatocellular carcinoma (18). Recently, the ability of ROS generation to suppress osteosarcoma has been reported (16). However, the role of ROS in the anticancer effect of pimozide in prostate cancer is not well known. In this study, we demonstrated that pimozide affects prostate cancer cells via oxidative stress. Our work is the first study to provide empirical evidence that pimozide inhibits prostate cancer through generating ROS.

2 MATERIALS AND METHODS

2.1 Reagents

Human prostate cancer cell lines PC-3 and DU145, and African green monkey kidney-derived Vero cell were acquired from the American Type Culture Collection (Manassas, VA, USA). Rat prostate cancer cell line AT-2 was obtained from Korean Cell Line Bank (KCLB, Seoul, South Korea). PC-3, DU145 and AT-2 cells were cultured in RPMI 1640 medium (Welgene, Gyeongsan, South Korea) supplemented with 10% fetal bovine serum (Gibco, Grand Island, NY, USA) and 1% penicillin/streptomycin (Gibco) at 37℃ in 95% air/5% CO2. Vero cell was cultured in DMEM medium (Welgene) supplemented with 10% FBS and 1% PS at 37℃ in 95% air/5% CO2. Pimozide (Sigma, St. Louis, MO, USA) was dissolved in dimethyl sulfoxide (DMSO) (Duksan Pure Chemical Co., Ansan, South Korea) to obtain concentration of 25 mM. Diphenylene iodonium (DPI) (Sigma) was dissolved in DMSO to obtain concentration of 10 mM. The final DMSO concentration in the culture media was 0.1%. DMSO at the same final concentration of 0.1% was used as control. Glutathione (GSH) (Sigma) was dissolved in distilled water to obtain concentration of 100 mM. Same distilled water was used as control.

2.2 Cell proliferation assay

Cells (1.6 × 104) were seeded in 96-well plates in 200 ㎕ media. The protocol for MTT assays was as described previously (95). The IC50 was calculated using

computer program GraphPad Prism 5 (GraphPad Software, La Jolla, CA, USA) with nonlinear regression (log[inhibitor] vs. response - Variable slope).

2.3 Clonogenic assay

Diluted 1 000 cells were seeded with culture medium in six-well plates and cultured for 7 days. Colonies were stained with 1% crystal violet (Merck, Darmstadt, Germany) and at least 50 cells were counted.

2.4 Scratch assay

Cell motility was analyzed using an in vitro scratch assay. PC-3 and DU145 cells were seeded into 6-well cell culture plate (SPL) and grown to 90% or above confluence. Monolayers of prostate cells were then scratched using a pipette tip. The migration areas were measured using Image J software (https://imagej.nih.gov/ij/).

2.5 ROS measurement in cell

The generation of intracellular ROS was determined using 2',7'-dichlorofluorescin diacetate (DCFH-DA) (Sigma) which is converted to fluorescent 2',7'-dichlorofluorescin in the presence of peroxides. After exposure to different concentrations of pimozide and GSH for 24 h, PC-3 and DU145 cells were treated with 10 μM DCFH-DA for 30 min at 37℃ and washed with PBS. The cells were detached with trypsin-EDTA (Gibco), and intracellular ROS was detected using a fluorescence

spectrometer Victor 3 (Perkin Elmer, Waltham, MA, USA) at 485 nm exposure and 535 nm emission.

2.6 Real-time reverse transcription-polymerases chain reaction (PCR)

Total RNA was extracted using a Hybrid-R RNA extraction kit (GeneAll Biotechnology, Seoul, South Korea). cDNA was synthesized by M-MLV cDNA Synthesis kit (Enzynomics, Daejeon, South Korea) according to the supplier's instructions. Quantitative real-time PCR was performed using TOPrealTM qPCR 2X PreMIX (Enzynomics) on a CFX Connect Real-Time PCR Detection system (Bio-Rad Laboratories, Hercules, CA, USA). Primers used were 5'-AGGGCATCATCAATTTCGAG-3' (sense) and 5'-TGCCTCTCTTCATCCTTTGG-3' (antisense) for human SOD1 (NCBI gene ID: 6647); 5'-GTGTGATGGTCCTTCCAACC-3' (sense) and 5'-CTGACATCCTCTGGCTCACA-3' (antisense) for human Prdx6 (NCBI gene ID: 9588); 5'-CAGTCTCAAGTATGTCCGT-3' (sense) and 5'-AGGCTCAATGTTGATGGT-3' (antisense) for human Gpx2 (NCBI gene ID: 2877); 5'-TTGGCTACCTTGCAGTTCGT-3' (sense) and 5'-ATGTGAACCATCGCAGGCA-3' (antisense) for human CISD2 (NCBI gene ID: 493856); 5'-CATGTACGTTGCTATCCAGGC-3' (sense) and 5'-CTCCTTAATGTCACGCACGAT-3' (antisense) for human β-actin (NCBI gene ID: 60). Ratio of target gene fold-change was normalized to human β-actin expression using comparative CT (2-ΔΔCt) method.

2.7 Animals

The experimental protocol for animal handling was in accordance with the National Institute of Health (NIH) guidelines and approved by the Institutional Animal Care and Use Committee of Seoul National University (Protocol Number: SNU-181128-1). Male TRAMP mice expressing the SV40 large T-antigen under control of the prostate-specific rat probasin promoter were purchased from The Jackson Laboratory (Bar Harbor, ME, USA) and housed in the Animal Experiment Facility, College of Veterinary Medicine, Seoul National University. Mice were kept on a 12-hr light/dark cycle with ad libitum access to food and water. Pimozide was suspended in 10% DMSO, 10% Tween80 (Sigma), and 80% PBS (Biosesang, Seongnam, South Korea). The mice were randomly assigned to control and treatment groups (n=5 for control and pimozide 10 mg/kg groups, and n=3 for pimozide 5 mg/kg group). Pimozide at 5 and 10 mg/kg/5 times per week was administered by intraperitoneal injection to TRAMP males beginning at 12 weeks of age and was continued until the animals were 24 weeks old at which time the experiment was terminated. Body weight was measured weekly.

2.8 Tissue Excision and Processing

At the time of sacrifice, the genitourinary tract (GUT: prostate, bladder, and seminal vesicle) were quickly excised and weighed. The anterior prostate lobes were dissected with inverted microscope (Olympus IX70), from one side and frozen in liquid nitrogen for ROS measurement and superoxide dismutase (SOD) assay. The remainder of each prostate was fixed in 10% buffered formalin and processed for standard paraffin sections.

2.9 Histopathological Analysis

The mouse prostate were identified histopathologically in H&E-fixed sections using previously published criteria (96, 97). Briefly, we evaluated each prostate and assigned low-grade, moderate-grade, and high-grade prostate intraepithelial neoplasia (PIN), phyllodes-like tumor, well-differentiated adenocarcinoma , moderately differentiated adenocarcinoma, or poorly differentiated adenocarcinoma grade, based on the most severe lesion and most common lesions within the prostate. The distribution of lesions was also estimated as focal, multifocal, or diffuse. The distribution and lesion grade were then combined to calculate a distribution-adjusted histopathological score ranging from 0 to 42, which could be used for statistical analysis. Sections were examined in a blinded manner under light microscopy (Olympus AX70, Tokyo, Japan).

2.10 ROS measurement in tissue

The quantitative measurement of ROS generation in prostate was performed with a slightly modified DCFH-DA method (98). The prostate samples were minced and homogenized in ice-cold PBS. The homogenates were centrifuged at 3,070 rpm for 10 min, the supernatants were re-centrifuged at 13,720 rpm for 20 min, and then the pellet, which contained mitochondria, was resuspended ice-cold PBS. All of manipulations above were carried out at 4℃. The DCFH-DA solutions at a final concentration of 2 μM were incubated for 30 min at 37℃. Fluorescence of samples was detected using a fluorescence spectrometer Victor 3 at 485 nm exposure and 535 nm emission.

2.11 SOD assay

Prostate tissue was dissected immediately and homogenized in ice-cold phosphate buffer. The homogenate was centrifuged, and the supernatant was used in the assay of SOD activity. SOD activity was determined according to the technical manual of the SOD assay kit-WST (Dojindo Molecular Technology Inc., Kumamoto, Japan).

2.12 Statistical analysis

All data are presented as mean ± standard error. Statistical significance ($P < 0.05$) was further analyzed with Student's t-test using computer program GraphPad Prism 5.

3 RESULTS

3.1 Pimozide inhibits cell proliferation and colony formation in the PC3 and DU145 cell lines

We analyzed the effect of pimozide on cell proliferation and colony formation. Treating human prostate cancer PC3 and DU145 cells, and rat prostate cancer AT-2 cells, with various concentrations of pimozide inhibited cell proliferation in a concentration-dependent manner (Fig. 1A). As a negative control for prostate cancer, Vero cells (derived from the African green monkey) were also treated with pimozide. There was no effect on the proliferation at concentrations below 25 μM. Based on these results, the half maximal effective concentrations (EC50) of pimozide were determined to be 16.43 μM and 11.53 μM in PC3 and DU145 cells, respectively (Fig. 1B). Pimozide also inhibited colony formation in PC3 and DU145 cells (Fig 1C); surviving colony counts are plotted in Figure 1D.

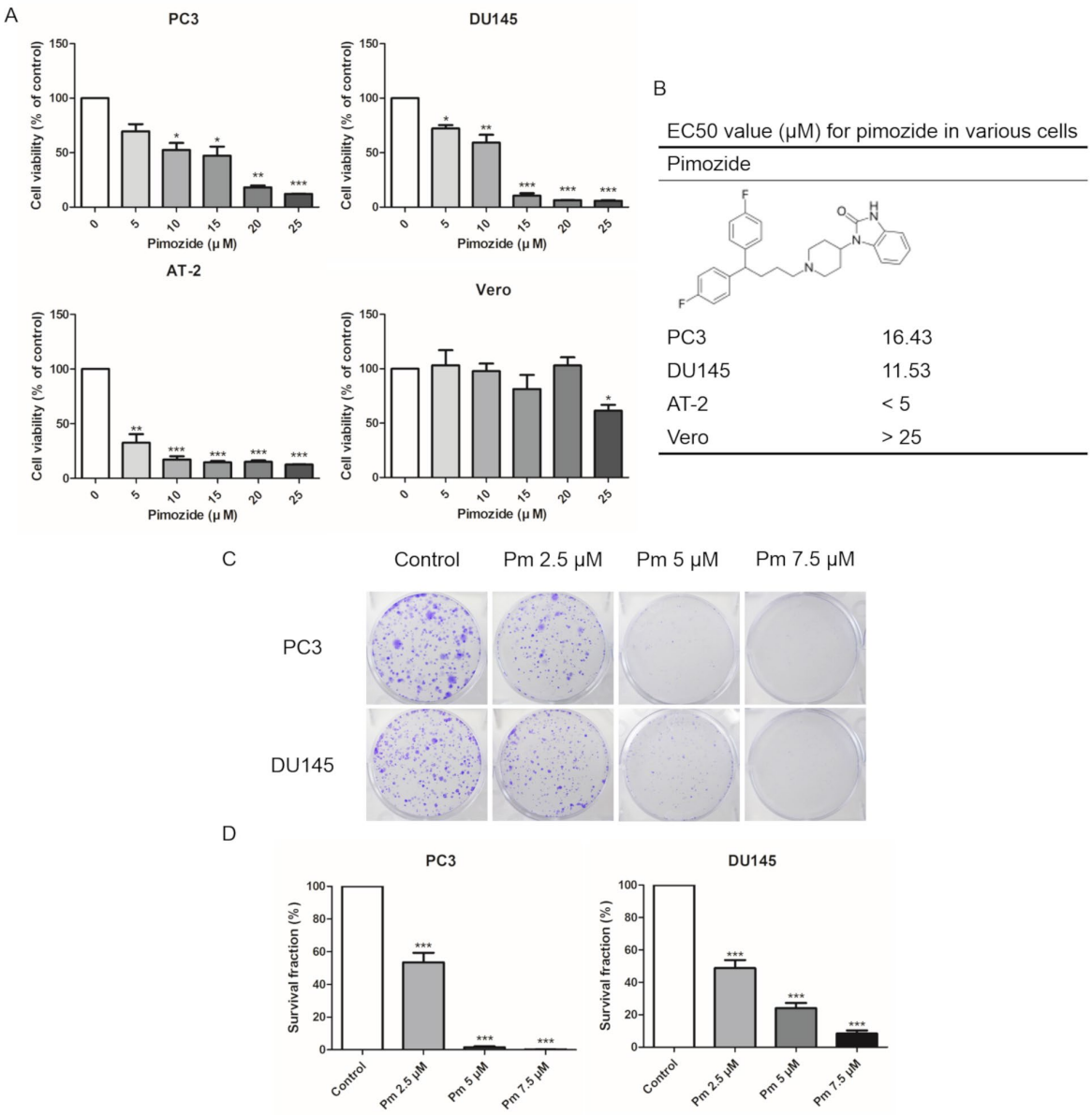

Fig. 1 The effect of pimozide on cell proliferation. (A) The inhibition of proliferation of PC3, DU145, AT-2 and Vero cells by pimozide was confirmed by MTT assay. (B) The structure of pimozide and estimated EC50 value for pimozide in various cells. The effect of pimozide on colony formation. (C) Colony formation of prostate cancer cell lines was inhibited in a concentration-dependent manner. (D) Surviving colony counts are plotted. *P<0.05; **P<0.01; ***P<0.001. Results are presented as means ± SEM.

3.2 Pimozide inhibits migration of PC3 and DU145 cells

We evaluated the migration PC3 and DU145 cells treated with pimozide by the scratch assay. After a 24 h treatment with various concentrations of pimozide, cell migration into the scratched area was inhibited in a concentration-dependent manner (Fig. 2A). The degree of migration was analyzed quantitatively and the results are shown in Figure 2B.

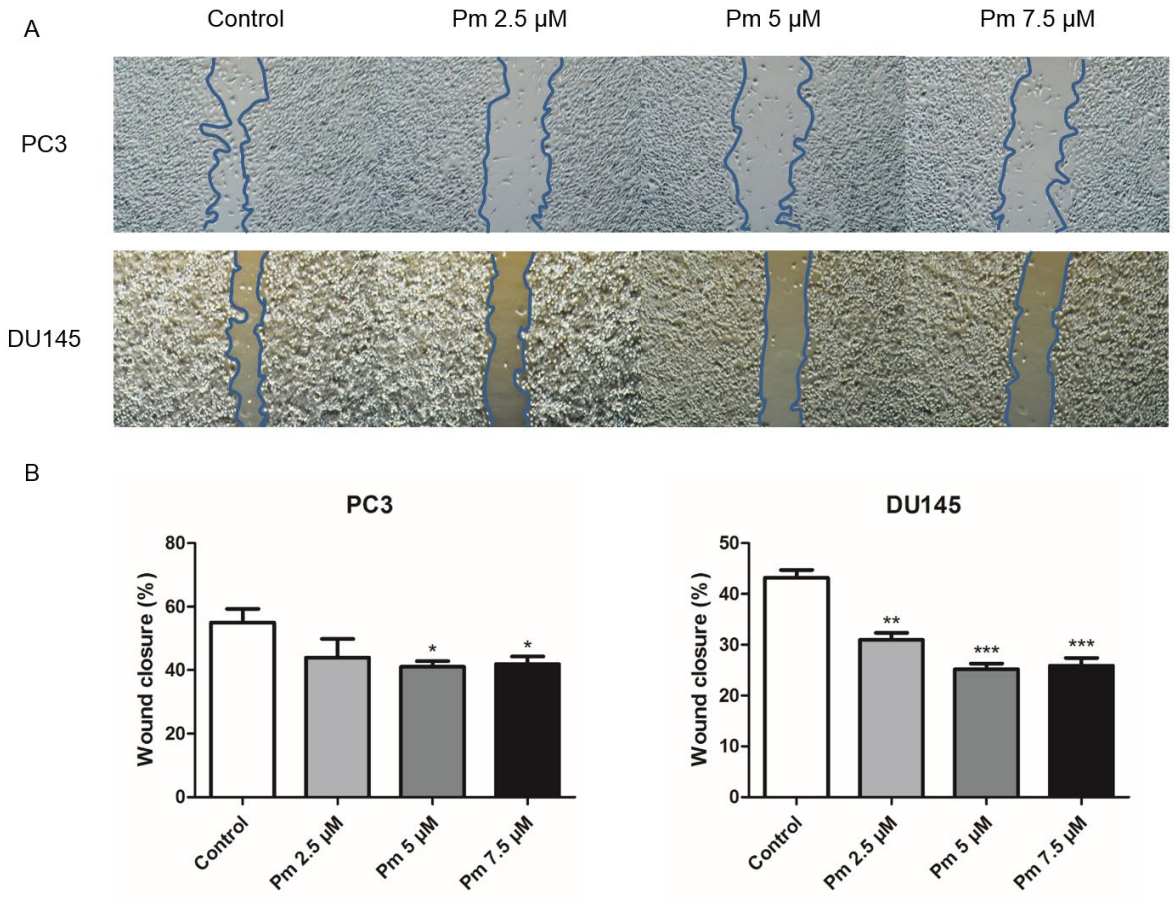

Fig. 2. The effect of pimozide on migration of PC3 and DU145. (A) Pimozide suppressed the migration of PC3 and DU145 human prostate cancer cells. (B) Cells that migrated to the migration area were photographed (magnification, x40). *P<0.05; **P<0.01; ***P<0.001. Results are presented as means ± SEM.

3.3 Pimozide inhibits the proliferation of PC3 and DU145 cells through ROS accumulation, which was inhibited by the antioxidant GSH

ROS accumulation affects cell proliferation. We treated PC3 and DU145 cells with various concentrations of pimozide and measured ROS present in the cells after 24 h using the fluorescent dye, DCFH-DA. As expected, treatment of both cell lines with pimozide increased the production of ROS (Fig. 3A). We also investigated whether the production of ROS by pimozide was related to its ability to inhibit the proliferation of prostate cancer cells. When PC3 and DU145 cells were treated with 15 μM pimozide (which increased ROS production compared to the control group) and 100 μM GSH, ROS levels decreased compared with cells treated with pimozide alone (Fig. 3B). Furthermore, the presence of 200 μM GSH reduced, to some extent, the pimozide-mediated inhibition of proliferation (Fig. 3C). NADPH oxidase is known as a major source of ROS (99). Treatment with DPI, an inhibitor of NADPH oxidase, decreased ROS production in pimozide-treated cancer cells (Fig. 3D).

The mRNA expression of SOD1, Prdx6, Gpx2, and CISD2 was analyzed after treatment of PC3 and DU145 cells with pimozide at concentration of 5, 10, and 15 μM for 24 h (Fig. 3E). Pimozide treatment reduced expression of the antioxidant enzymes SOD1, Prdx6, and CISD2 (which regulates the accumulation of ROS). However, mRNA expression of Gpx2 increased.

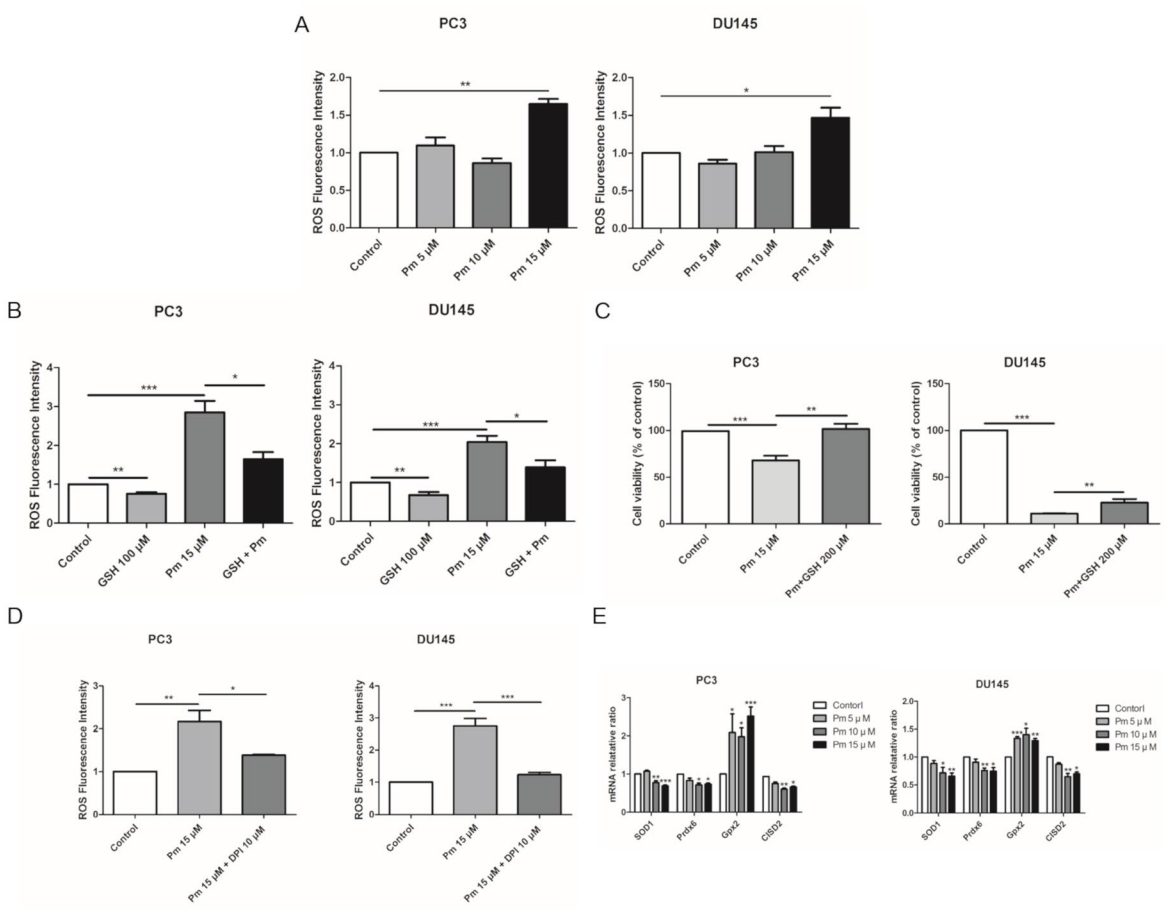

Fig. 3 The effect of pimozide on the prostate cancer cells is related to ROS generation. (A) Pimozide induced generation of ROS in the PC3 and DU145 cells. Fluorescence spectrometer was used to determine ROS generation after staining with DCFH-DA. (B) ROS generation by pimozide was inhibited by the antioxidant GSH. (C) The inhibition of proliferation by pimozide was inhibited by the antioxidant GSH. Cell proliferation was confirmed by MTT assay. (D) The pimozide-induced ROS was inhibited by DPI. (E) Pimozide downregulated the mRNA expression levels of anti-oxidant enzymes SOD1, Prdx6 and upregulated the mRNA expression levels of anti-oxidant enzyme Gpx2 in PC3 and DU145 cells. The mRNA expression levels of CISD2 was downregulated in PC3 and DU145 cells. *P<0.05; **P<0.01; ***P<0.001. Results are presented as means ± SEM.

3.4 Pimozide inhibits prostate cancer development in TRAMP mice through the generation of ROS

TRAMP mice show morphological and histological characteristics of human prostate cancer (100). We administered pimozide of 5 mg/kg and 10 mg/kg or vehicle to TRAMP mice and observed no noticeable toxicity or clinical symptoms during the treatment. All mice were necropsied after 12 weeks of treatment to grossly confirm the development of prostate cancer (Fig. 4A, B). After 12 weeks of pimozide administration, there were no significant changes in body weight (Fig. 4C).

The prostate of TRAMP mice treated with pimozide was examined histopathologically. Representative histologic photographs are presented at magnifications of 100x and 400x in Figures 5A-F. In control untreated mice, poorly differentiated adenocarcinomas with irregular cytoplasm and nuclei were observed (Fig. 5A, D). High-grade PIN (arrow), which almost completely filled the lumen of the prostate, was mainly observed in the 5 mg/kg pimozide group (Fig. 5B, E). In the 10 mg/kg pimozide group, moderate-grade PIN (arrow) with epithelial cell proliferation was observed (Fig. 5C, F). Histopathological scores were decreased in a dose-dependent manner in the pimozide-treated groups (Fig. 5G). The ROS level, measured using DCFH-DA in the anterior lobe of the prostate, was higher in mice treated with pimozide than control mice (Fig. 5H). SOD activity, measured in the anterior lobe of the prostate, was decreased in pimozide-treated mice compared to controls (Fig. 5I).

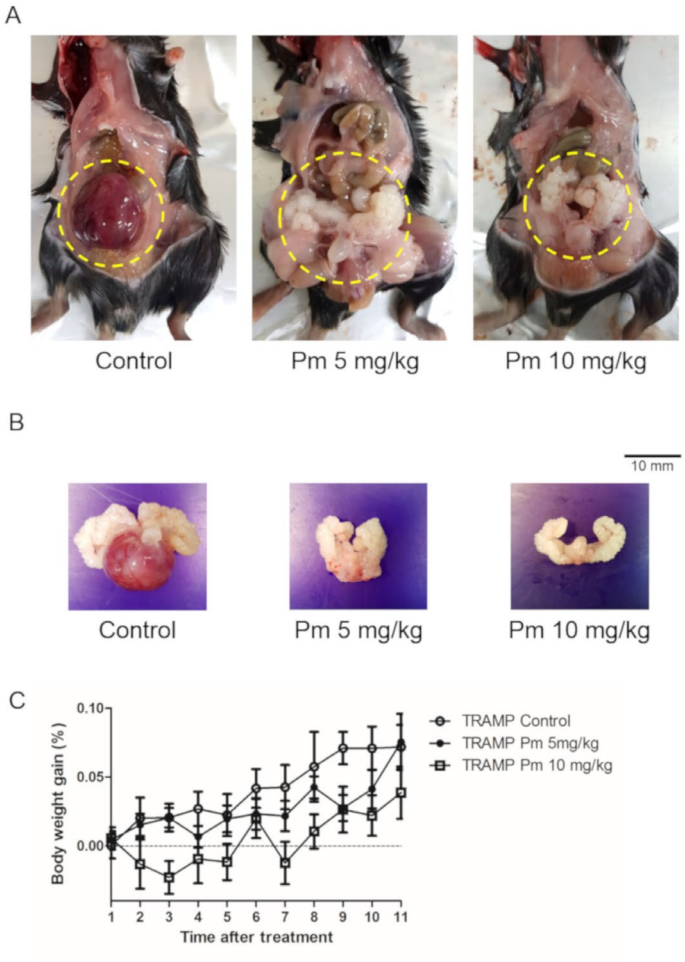

Fig. 4 Effect of pimozide administration on prostate cancer progression in TRAMP mice. Pimozide was administered at 5 and 10 mg/kg/5 times per week by intraperitoneal injection beginning at 12 weeks of age for 12 weeks. (A) Representative pictures of dissected control and pimozide-treated TRAMP mice at 24 weeks of age. (B) Representative pictures of excised GUT from control and pimozide-treated TRAMP mice at 24 weeks of age. (C) Body weight gain profile of control and pimozide-treated TRAMP mice recorded weekly.

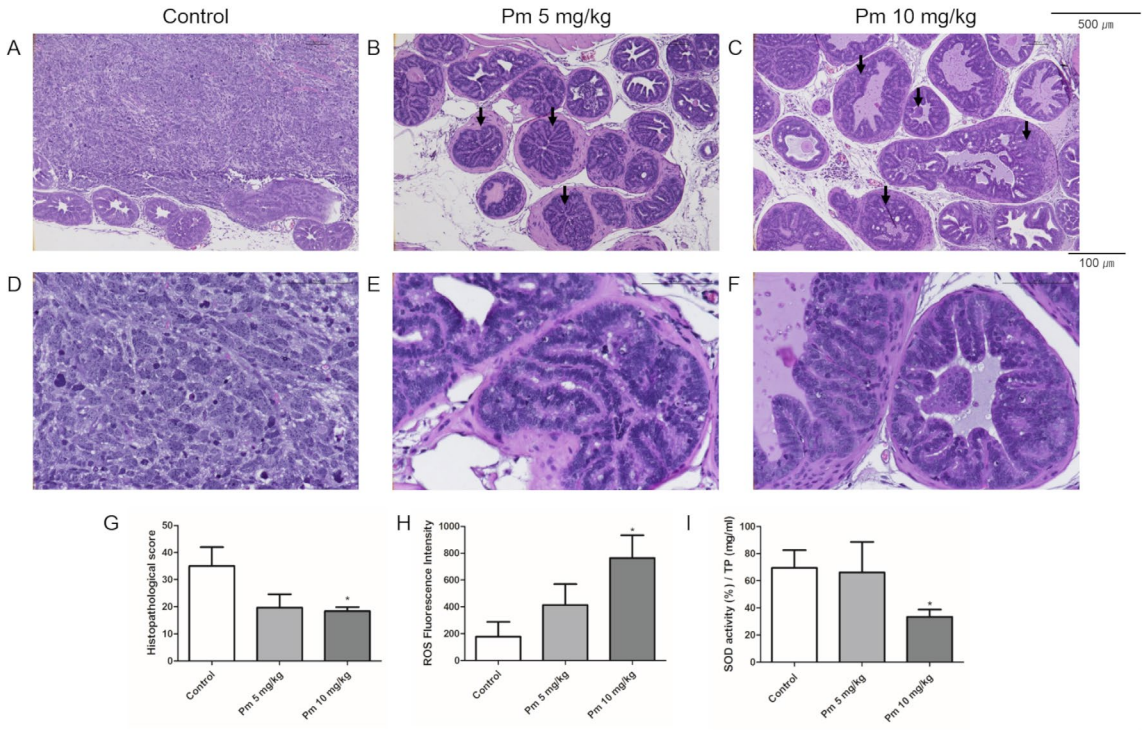

Fig. 5 Effect of pimozide administration on prostate cancer progression in TRAMP mice. (A and D) Control TRAMP mice exhibited poorly differentiated adenocarcinoma with high mitotic index, frequent nuclear and cytoplasmic atypia, and the lack of glands (H&E, A x100; D x400). (B, C, E, and F) Administration of pimozide resulted in a marked reduction in adenocarcinoma and cribriform structure of epithelium with moderate and high-grade PIN (arrow) (H&E, B and C x100; E and F x400). (G) Histopathologic score was evaluated in TRAMP mice. Pimozide reduced histopathologic score. (H) Pimozide induced generation of ROS in the anterior lobes of prostate in TRAMP mice. (I) Pimozide inhibited the activity of anti-oxidant enzyme SOD in the anterior lobes of prostate in TRAMP mice. *P<0.05. Results are presented as means ± SEM.

4 DISCUSSION

Because of the limited success of current prostate cancer therapies, there is a growing demand for candidates for new prostate cancer treatments through drug repurposing. One possibility is pimozide, a United States Food and Drug Administration-approved antipsychotic drug that has therapeutic effects in many cancers (10, 16, 18). In the current study, we report that pimozide inhibits the proliferation of PC3, DU145, and AT-2 prostate cancer cells. Importantly, this effect appears to be specific to cancer cells because the proliferation of Vero cells, a normal line derived from African green monkey (79, 95), was unaffected by pimozide at concentrations below 25 μM. This finding is consistent with a report that pimozide is specific for hepatocellular carcinoma (15).

We confirmed that the anticancer effect of pimozide was related to ROS generation as reported previously (16). Antioxidants have been reported to inhibit ROS-based anticancer effects (101). Treatment with DPI, an inhibitor of NADPH oxidase, inhibited ROS production by pimozide. This means that NADPH oxidase is partially involved in ROS generation by pimozide. To determine whether ROS produced by pimozide were involved in its anticancer effect, GSH, an antioxidant, was administered. GSH decreased the ROS produced by pimozide and prevented the pimozide-mediated inhibition of proliferation of prostate cancer cells. The restoration of cell viability by GSH in presence of pimozide looks much weaker in DU145 compared to PC3. PC3 is a prostate cancer cell line with higher malignancy than DU145, and this difference appears to be the results (102). This suggests that ROS play an important role in the anticancer mechanism of pimozide.

CISD2 belongs to the CDGH iron sulfur domain-containing family (83). CISD2 inhibits ROS production in lung cancer, which is reportedly associated with a poor prognosis of lung adenocarcinoma (86). In the current study, pimozide reduced the expression of CISD2 and the antioxidant enzymes SOD1 and Prdx6, which might have augmented ROS levels. In contrast, the expression of Gpx2 increased and GSH treatment decreased the expression. This may be because, under oxidative stress conditions, Nrf2 increases the expression of antioxidant enzymes and Gpx2 is a target of Nrf2 (103). Overall, pimozide increased the production of ROS in prostate cancer cells and inhibited their proliferation by overcoming the antioxidant enzyme capacity.

TRAMP mice are a suitable animal model of human prostate cancer. In this mouse, prostate cancer occurs spontaneously and shows the histological and molecular characteristics of human prostate cancer (100). We have shown that the histological scores were decreased in TRAMP mice treated with pimozide. In addition, it was demonstrated that there were no significant changes in body weight indicating clinical symptoms following treatment. There was no significant difference in the weight of GUT (unpublished data).

Through the experiments reported here, we confirmed that pimozide plays an important role in the inhibition of prostate cancer in vitro by producing ROS and, importantly, that this effect can be reproduced in vivo. Increased ROS production was observed in the anterior prostate of pimozide-treated mice. We also confirmed that the activity of SOD, an antioxidant enzyme, was decreased. Based on these results, we hypothesized that pimozide formed ROS in TRAMP mice and decreased the activity of antioxidant enzymes. Thus, the ROS level exceeded the ability of prostate cancer cells to remove them and inhibited the cancer.

These results may be interpreted as contradictory to previous reports that ROS induce prostate cancer. However, it is necessary remember that ROS play different roles at different levels and in different stages of the tumor (104). For example, ROS can induce DNA damage at early times to promote cancer initiation, but higher levels of ROS can induce apoptosis thereby inhibiting cancer (4). In the control group with prostate cancer, the ROS level was lower than in the pimozide-treated group without prostate cancer, suggesting that above a certain level ROS inhibited cancer. However, the level of ROS in the control group is expected to be higher than that of non-transgenic littermates that do not develop prostate cancer.

The results of this study suggest that pimozide has a therapeutic effect on prostate cancer in vivo and in vitro. The mechanism by which pimozide inhibits prostate cancer appears to be associated with increased ROS production. Co-treatment with pimozide and the antioxidant, GSH, decreased ROS levels and the anticancer effect of pimozide. In vivo, prostate cancer was reduced in TRAMP mice treated with pimozide, and this effect was associated with increased ROS. Thus, we suggest pimozide as a promising anticancer therapy agent.

CHAPTER III

Down regulation of glutathione peroxidase 3 induces ROS and contributed to prostate hyperplasia in *Nkx3.1* knockout mice

1 INTRODUCTION

Prostate cancer is the most commonly diagnosed non-skin cancer in men in the US and is the leading cause of cancer-related death (1). In 2019, 174,650 people will be diagnosed with prostate cancer in the US and 31,620 are expected to die (2). Prostate cancer is age-related, and increasing reactive oxygen species (ROS) play an important role in the development and progression of prostate cancer (3). ROS assists cancer cell proliferation, invasion and metastasis and inhibits apoptosis, leading to cancer progression (4).

NKX3.1 is an androgen-related gene and encodes a homeobox protein that acts as a tumor suppressor in prostate cells (105, 106). *NKX3.1* loss has been reported in human prostate cancer. In humans, the loss of heterozygosity of *NKX3.1* in early stages of prostate cancer has been observed in significant proportions (107, 108). Loss of *Nkx3.1* in mice causes developmental problems such as ductal branching morphogenesis, secretory protein production, and growth in the prostate (109, 110). In addition, *Nkx3.1* knockout mice develops prostatic intraepithelial neoplasia (PIN), a pre-cancerous lesion (111). Although the loss of *Nkx3.1* does not lead to invasive carcinoma, it is known that additional loss of cancer suppressor genes such as *Pten* cause invasive adenocarcinoma and metastasis (112). It was reported that oxidative stress in the progression of prostate cancer is related to *Nkx3.1* (87).

Oxidative stress contributes to cancer initiation, advancement, and progression (19). Under normal physiological conditions, cells have sufficient antioxidant capacity to eliminate ROS (20). However, increased ROS production or decreased antioxidant activity can lead to chronic oxidative stress. Glutathione peroxidase (GPX) is present in various tissues (66, 67, 113), (66, 67, 113), and plays

an important role in ROS elimination. Four types exist: cellular GPX1, gastrointestinal GPX2, extracellular GPX3, and phospholipid hydroperoxide GPX4, which are structurally, and functionally different (68). GPX3 plays an important role in ROS elimination. Silencing *Gpx3* expression was reported to enhance metastasis of human thyroid cancer cells and gastric cancer cells (21, 22). Inflammatory colorectal cancer was induced in *Gpx3* knockout mice, and it was reported to increase inflammation, proliferation, and DNA damage. In addition, the expression of genes associated with oxidative stress was altered, which means that GPX3 plays an important role in the development of tumors as a ROS scavenger (23). Several studies reported that GPX3 is associated with Wnt/β-catenin signaling (21, 23) or p53-induced gene 3 signaling (69).

We have previously reported an increase in prostate cancer growth following GPX3 inhibition in transgenic adenocarcinoma of the mouse prostate (TRAMP) mice (82). This means that GPX3 deficiency plays an important role in the development of prostate cancer. We hypothesized that GPX3 might play an important role in the development of PIN, the pre-cancerous stage of prostate cancer, and hyperplasia of the prostate gland. Although TRAMP mice develop adenocarcinoma via PIN, there is a concern that TRAMP mice are a model using exogenous oncogene SV40 T antigen which does not exist in humans (114). Therefore, we made *Nkx3.1; Gpx3* knockout mice developing PIN to see how *Gpx3* loss affects PIN. Our data showed that *Gpx3* loss causes oxidative stress in the prostate gland and contributes to the hyperplasia of PIN, a prerequisite for prostate cancer, and further suggest that it play an important role in the development of prostate cancer.

2 MATERIALS AND METHODS

2.1 Cell cultures

Human prostate cancer cell lines PC3 was acquired from the American Type Culture Collection (Manassas, VA, USA). The non-tumorigenic human prostate epithelial cell line RWPE-1 was received from Dr. Won-Woo Lee (College of Medicine, Seoul National University, Seoul, South Korea). Normal prostate cell line WPMY-1 was received from Dr. So Yeong Lee (College of Veterinary Medicine, Seoul National University, Seoul, South Korea). PC-3 and WPMY-1 cells were cultured in RPMI 1640 medium (Welgene, Gyeongsan, South Korea) supplemented with 10% fetal bovine serum (Gibco, Grand Island, NY, USA) and 1% penicillin/streptomycin (Gibco) at 37℃ in 95% air/5% CO2. The RWPE-1 cells were cultured in keratinocyte serum-free medium (KSFM; Gibco) supplemented with 50 mg/L bovine pituitary extract and 5 μg/L epidermal growth factor (EGF; Gibco).

2.2 ROS measurement in cell

The generation of intracellular ROS was determined using 2',7'-dichlorofluorescin diacetate (DCFH-DA) (Sigma, St. Louis, MO, USA) which is converted to fluorescent 2',7'-dichlorofluorescin in the presence of peroxides. Cells were treated with 10 μM DCFH-DA for 30 min at 37℃ and washed with PBS. The cells were detached with trypsin-EDTA (Gibco), and intracellular ROS was detected using a fluorescence spectrometer Victor 3 (Perkin Elmer, Waltham, MA, USA) at 485 nm exposure and 535 nm emission.

2.3 Cell proliferation assay

The proliferation capacity of cells was analyzed using thiazolyl blue tetrazolium bromide (MTT) (Sigma) assay based on the ability of live cells to convert tetrazolium salt into purple formazan. Briefly, cells were seeded into 96-well cell culture plates (SPL Life Science, Pocheon, South Korea) at a density of 1.6 x 10^4 per well in 200 ㎕ media. After 24 h of culturing, the medium was replaced to FBS free media for 24 h. Cells were treated with hydrogen peroxide (H_2O_2) (30%, Junsei, Tokyo, Japan) at concentration of 0.1, 0.5, 1, 5, and 10 μM or vehicle (distilled water) control and cultured for 24 h. The medium was then changed with 100 ㎕ of MTT (diluted to 0.5 mg/ml in FBS-free medium from a stock solution of 5 mg/ml) and incubated at 37℃ for 3 h. The supernatant was eliminated and 100 ㎕ of dimethyl sulfoxide (DMSO) (Duksan Pure Chemical Co., Ansan, South Korea) was supplemented to each well to dissolve the formazan crystals. Plates were agitated at room temperature for 5 min. The absorbance was read at 570 nm on an Epoch BioTek microplate reader (BioTek, Winooski, VT, USA). All treatments were performed in triplicates.

2.4 Animals and PCR genotyping

All animal studies were approved by the Institutional Animal Care and Use Committee of Seoul National University (Protocol Number: SNU-161201-2-3). Parental Gpx3 KO mice created in a C57BL/6 background were previously described (115). GPx3 KO mice obtained from Dr. Raymond F. Burk (Department of Medicine, Vanderbilt University School of Medicine, Nashville, TN). Parental Nkx3.1 mice

created in a C57BL/6 background was obtained from Dr. Jeffrey Milbrandt (Department of Genetics, Washington University School of Medicine, St. Louis, MO) (111). The mice were housed in the Animal Experiment Facility, College of Veterinary Medicine, Seoul National University. Mice were kept on a 12-hr light/dark cycle with ad libitum access to food and water. *Nkx3.1*$^{-/-}$ KO mice were bred with *Gpx3*$^{+/-}$ KO mice to generate *Nkx3.1*+/-; *Gpx3*+/+ and *Nkx3.1*+/-; *Gpx3*+/- mice. Then, *Nkx3.1*-/-; *Gpx3*+/+, *Nkx3.1*-/-; *Gpx3*+/-, and *Nkx3.1*-/-; *Gpx3*-/- mice were generated through backcross and sibling breeding. PCR genotyping was performed as described previously (111, 115). The number of mice in each experimental group was 4-8.

2.5 Tissue excision and processing

Mice were sacrificed at approximately 4, 8, and 12 month. The body weight were weighed and genitourinary tract (GUT: prostate, bladder, and seminal vesicle) were quickly excised and weighed. The ventral and dorsal prostate lobes were dissected with inverted microscope (Olympus IX70), from one side and frozen in liquid nitrogen for Real-time reverse transcription-polymerases chain reaction (PCR), ROS measurement, and superoxide dismutase (SOD) assay. The remainder of each prostate was fixed in 10% buffered formalin and processed for standard paraffin sections.

2.6 Real-time reverse transcription PCR

Total RNA was extracted using a Hybrid-R RNA extraction kit (GeneAll Biotechnology, Seoul, South Korea). cDNA was synthesized by M-MLV cDNA

Synthesis kit (Enzynomics, Daejeon, South Korea) according to the supplier's instructions. Quantitative real-time PCR was performed using TOPrealTM qPCR 2X PreMIX (Enzynomics) on a CFX Connect Real-Time PCR Detection system (Bio-Rad Laboratories, Hercules, CA, USA). Ratio of target gene fold-change was normalized to mouse β-actin expression using comparative CT (2-ΔΔCt) method.

Table 1. Gene-specific primers of mouse.

Human			
Genes	Forward	Reverse	NCBI gene ID
NKX3.1	GAGGCGAAAGCGGAGGG	CCGCAGGATGTCCTGGATG	4824
GPX3	ACATGCCTACAGGTATGCGT	GAGCAGAACAATTGGACCTA	2878
ACTB	CATGTACGTTGCTATCCAGGC	CTCCTTAATGTCACGCACGAT	60
Mouse			
Genes	Forward	Reverse	NCBI gene ID
Sod3	TTCTACGGCTTGCTACTGGC	GCTAGGTCGAAGCTGGACTC	20657
Gpx2	CTCAGTGTACCCTCGGGAGA	AAAGGAAATGGCCGGTAGGG	14776
Nos2	TGGTGAAGGGACTGAGCTGT	GCTACTCCGTGGAGTGAACA	18126
Hmox	AAGCTTTTGGGGTCCCTAGC	GGTGAGGGAACTGTGTCAGG	15368
Cisd2	TTGCACGGATAAGGACGAGG	AGGTCTTATCACTCGGGCCT	67006
Ctnnb1	GATATTGACGGGCAGTATGCAA	AACTGCGTGGATGGGATCTG	12387
Ccnd1	AGCAGAAGTGCGAAGAGG	GCAGTCAAGGGAATGGTC	12443
Axin2	GGCTGCGCTTTGATAAGGTC	CGCGAACGGCTGCTTATTTT	12006
Mmp7	ACTTCAGACTTACCTCGGATCG	TCCCCCAACTAACCCTCTTGA	17393
Myc	AAGGGAAGACGATGACGG	TGAGAAACCGCTCCACATA	17869
Foxa2	GAGCACCATTACGCCTTCAAC	AGGCCTTGAGGTCCATTTTGT	15376
Tcf4	TGCCGACTACAACAGGGACT	TGCTGGACTGTGGGATATGA	21413

Twist1	CACGCTGCCCTCGGACAA	GGGACGCGGACATGGACC	22160
Actb	GTCCCTCACCCTCCCAAAAG	GCTGCCTCAACACCTCAACCC	11461

2.7 ROS measurement in prostate tissues

The generation of intracellular ROS was determined using 2',7'-dichlorofluorescin diacetate (DCFH-DA) (Sigma) which is converted to fluorescent 2',7'-dichlorofluorescin in the presence of peroxides. The quantitative determination of ROS production was performed with a slightly modified DCFH-DA method (98, 116). The prostate tissues were minced and homogenized in ice-cold phosphate-buffered saline (PBS) (pH 7.4). The homogenates were centrifuged at 3,070 rpm for 10 min, the supernatants were re-centrifuged at 13,720 rpm for 20 min, and then the pellet, which contained mitochondria, was resuspended in ice-cold PBS. All of the manipulations above were carried out at 4℃. The DCFH-DA solution at a final concentration of 2 μM and the resuspension were incubated for 30 min at 37℃. Fluorescence of the samples was detected using a fluorescence spectrometer Victor 3 (Perkin Elmer, Waltham, MA, USA) at 485 nm exposure and 535 nm emission.

2.8 SOD assay

Prostate tissue was dissected immediately and homogenized in ice-cold phosphate buffer. The homogenate was centrifuged, and the supernatant was used in the assay of SOD activity. SOD activity was determined according to the technical manual of the SOD assay kit-WST (Dojindo Molecular Technology Inc., Kumamoto, Japan).

2.9 Histopathological Analysis

The mouse prostate were identified histopathologically in H&E-fixed sections using previously published criteria (96, 97). Briefly, we evaluated each prostate and assigned low-grade, moderate-grade, and high-grade prostate intraepithelial neoplasia (PIN) based on the most severe lesion and most common lesions within the prostate. The distribution of lesions was also estimated as focal, multifocal, or diffuse. The distribution and lesion grade were then combined to calculate a distribution-adjusted histopathological score ranging from 0 to 42, which could be used for statistical analysis. Sections were examined in a blinded manner under light microscopy (Olympus AX70, Tokyo, Japan). The epithelium thickness was calculated by measuring the distance between the basal pole and the apical pole of the acini epithelium cells. Ten linear measurements were made in 3 distinct fields randomly distributed throughout the acini and expressed as μm. Lumen area analysis was performed in a microscopic magnification of 200x, where 3 acini per animal was selected and measured.

2.10 Statistical analysis

All data are presented as mean ± standard error. Statistical significance ($P < 0.05$) was further analyzed with Student's t-test using computer program GraphPad Prism 5 (GraphPad Software, La Jolla, CA, USA).

3 RESULTS

3.1 Oxidative stress promoted proliferation in normal prostate cell RWPE-1.

Reduced expression of *NKX3.1* and *GPX3* was reported in human prostate cancer (117, 118). We compared basal mRNA expression levels of *NKX3.1* and *GPX3* in normal prostate cells, WPMY-1 and RWPE-1, with cancer cell PC3 (Fig. 1A-B). The mRNA expression of *NKX3.1* in RWPE-1 was similar to WPMY-1, which was decreased in PC3. Similarly, *GPX3* showed similar levels in WPMY-1 and RWPE-1, which was decreased in PC3. Similarly, the basal levels of ROS were measured. ROS levels of RWPE-1 and WPMY-1 were similar, but increased significantly in PC3 (Fig. 1C). H_2O_2 was treated to determine the effect of oxidative stress on normal prostate cells, RWPE-1. H_2O_2 induced oxidative stress in RWPE-1 (Fig. 1D). Induced oxidative stress was found to promote proliferation of RWPE-1 (Fig. 1E). However, as the concentration of H_2O_2 increased, proliferation was decreased.

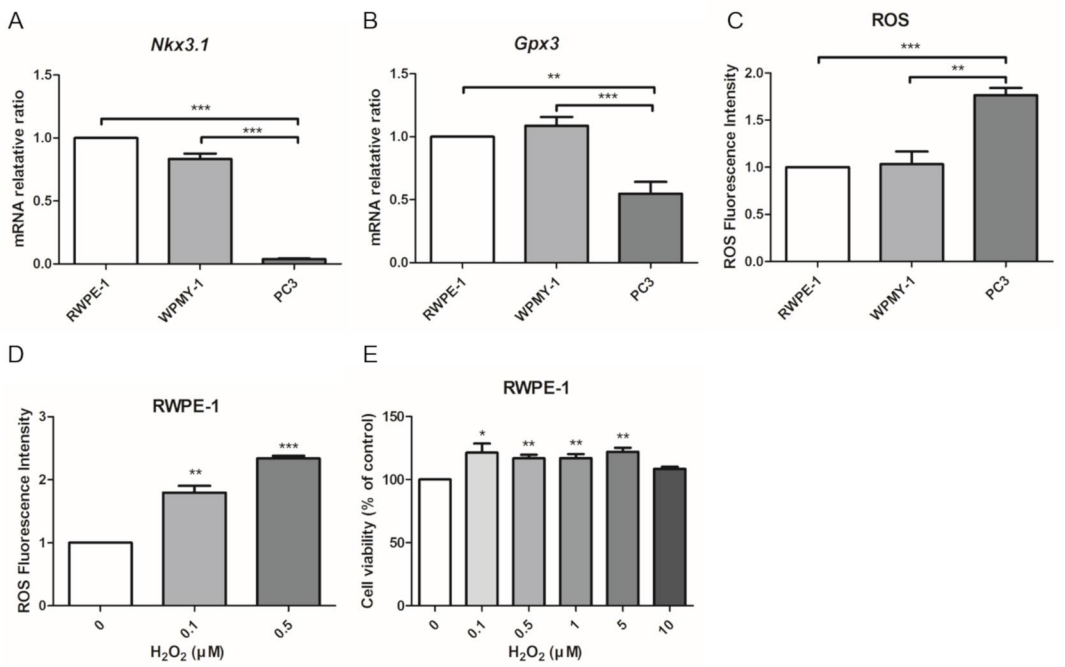

Fig. 1 Promoted proliferation by oxidative stress in normal prostate cells. (A) The basal mRNA expression of *NKX3.1* in prostate cancer cell PC3 and normal prostate cells RWPE-1 and WPMY-1 was analyzed by qPCR (n=3). (B) The basal mRNA expression of *GPX3* in prostate cancer cell PC3 and normal prostate cells RWPE-1 and WPMY-1 was analyzed by qPCR (n=3). (C) The basal levels of ROS in prostate cancer cell PC3 and normal prostate cells RWPE-1 and WPMY-1 was measured with DCFH-DA (n=3). (D) H_2O_2 was treated to induce ROS in RWPE-1 and ROS levels were measured with DCFH-DA (n=3). (E) H_2O_2 was treated to RWPE-1 for 24h and proliferation was measured by using MTT assay (n=3). **P*<0.05; ***P*<0.01; ****P*<0.001. Results are presented as means ± SEM.

3.2 *Gpx3* Knockout did not cause drastic changes in the prostate gland.

Genotypes of procured mice were confirmed by PCR. The bands of wildtype and knockout were identified for *Nkx3.1* and *Gpx3*, respectively. (Fig. 2A-B). *Nkx3.1*-/-; *Gpx3*+/+, *Nkx3.1*-/-; *Gpx3*+/-, and *Nkx3.1*-/-; *Gpx3*-/- mice were euthanized at 4, 8, and 12 months to observe the changes in the prostate gland. As a result of visual observation of the GUT, it was observed that the GUT size increased with age, but no difference was observed between *Gpx3* knockout groups (Fig. 2C). Body weight, GUT weight, and GUT weight/body weight increased with age, but no difference was observed between *Gpx3* knockout groups (Fig. 2D-F).

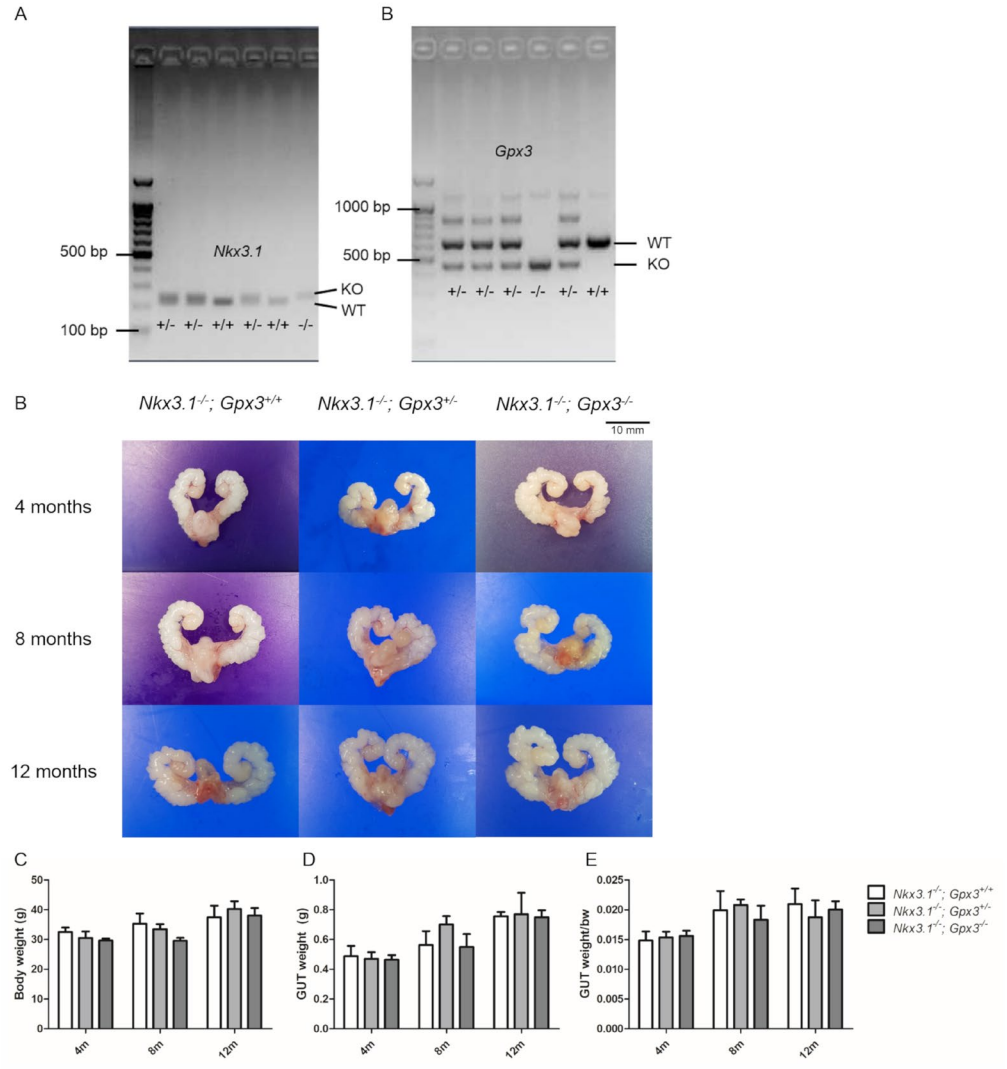

Fig. 2 Generation of *Nkx3.1; Gpx3* knockout mice and representative pictures of genitourinary tract and weighing results. (A) Agarose gel photograph of genotyping results of PCR products from *Nkx3.1*$^{+/+}$, *Nkx3.1*$^{+/-}$, *Nkx3.1*$^{-/-}$ mice. **(B)** Agarose gel photograph of genotyping results of PCR products from *Gpx3*$^{+/+}$, *Gpx3*$^{+/-}$, *Gpx3.1*$^{-/-}$ mice. **(C)** Mice were sacrificed at 4-month, 8-month, and 12-month old. The Representative images of genitourinary tract was taken after necropsy mice (n=4~8). **(D)** Body weight was measured before necropsy (n=4~8). **(E)** Genitourinary tract weight was measured after necropsy (n=4~8). **(F)** Genitourinary tract weight/body weight ratio was measured (n=4~8). GUT, genitourinary tract; bw, body weight

3.3 *Gpx3* knockout alters the expression of genes associated with oxidative stress but does not alter Wnt/β-catenin signaling.

GPX3 plays an important role in suppressing prostate cancer by removing ROS. We identified how *Gpx3* knockout affected mRNA expression of oxidative stress-related genes in the prostate (Fig. 3A). *Sod3* acts as an antioxidant by metabolizing extracellular superoxide produced by NADPH oxidase to H_2O_2 (119). Reduction of the expression of the antioxidant enzyme *Gpx2* was reported in previous *Nkx3.1* KO mice (87). *Hmox* is an antioxidant enzyme that regulates oxidative stress and is involved in tumorigenesis of prostate cancer (120). *Nos2* is a pro-oxidant gene, but expression has been reported to decrease with increasing ROS levels in cells (121). *CISD2* is a redox-sensitive gene. Overexpression of *CISD2* has been reported to be associated with increased antioxidant capacity against ROS (86). When *Gpx3* was knocked out, mRNA expressions of antioxidant enzymes *Sod3* and *Hmox* were increased at 4 months, and decreased at 8 and 12 months of age. The mRNA expression of antioxidant enzyme *Gpx2* decreased, at all ages. The mRNA expression of *Cisd2*, which regulates antioxidant capacity, increased at 4 months and decreased at 8 and 12 months. The mRNA expression of *Nos2* was increased at 4 months and decreased at 8 and 12 months, which appeared to be related with increasing ROS levels as mice age.

Inhibition of *Gpx3* has been reported to increase the expression of *Ctnnb1* and its targets (21, 82). We identified how *Gpx3* knockout affected the Wnt/β-catenin pathway (Fig. 3B). We confirmed the mRNA expression of *Ctnnb1* and its downstream targets; *Ccnd1*, *Axin2*, *Mmp7*, *Myc*, *Foxa2*, and *Tcf4*, but did not see the difference in all age groups. Wnt/β-catenin is also associated with epithelial mesenchymal transition

(EMT) in prostate cancer (65), but mRNA expression of *Twist1*, associated with EMT, was not changed.

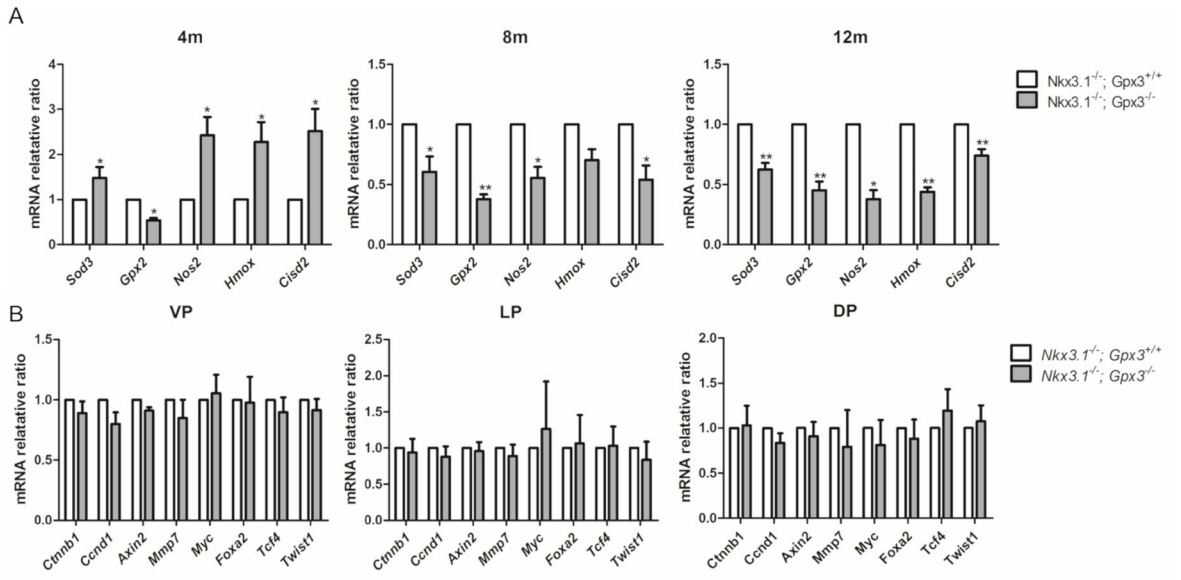

Fig. 3 The mRNA expression of prostate in *Nkx3.1*; *Gpx3* knockout mouse. (A) The mRNA expression of genes related to oxidative stress in ventral prostate of 4, 8, and 12 months old mice was analyzed by qPCR (n=4~8). (B) The mRNA expression of Ctnnb1 and its downstream signals in ventral prostate, lateral prostate, and dorsal prostate in 12-month-old mice was analyzed (n=4~8). *P<0.05; **P<0.01. Results are presented as means ± SEM.

3.4 *Gpx3* knockout increased ROS production and decreased SOD activity in the prostate.

We found that knocking out *Gpx3* reduced the expression of genes related to antioxidant activity. We further analyzed how these genetic changes affect oxidative stress in the prostate gland. At 12 months of age, ROS production increased in the *Gpx3* knockout group (Fig. 4A). We measured the activity of SOD, an antioxidant enzyme that eliminates oxidative stress. Its activity was found to decrease in 12-month-old *Gpx3* knockout mice (Fig. 4B).

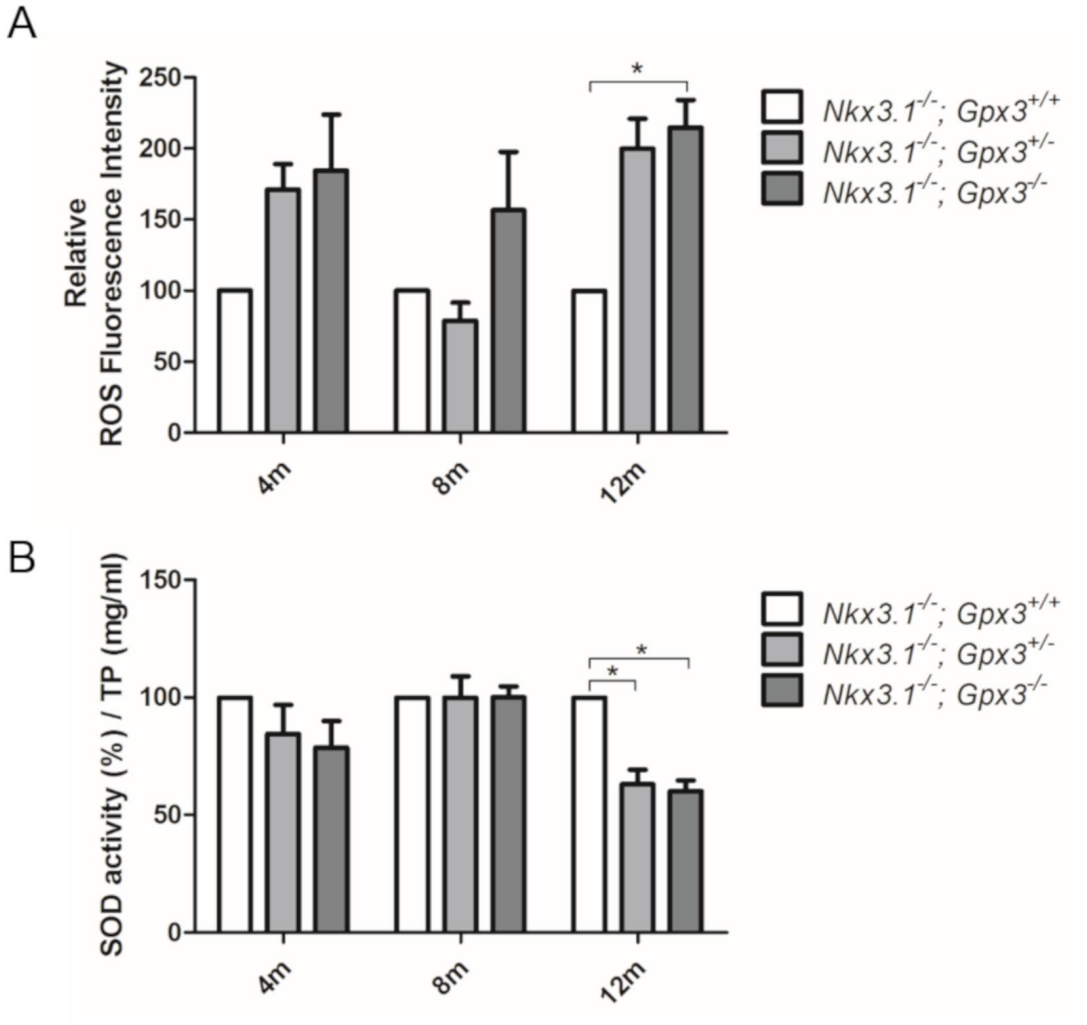

Fig. 4 ROS levels and antioxidant enzyme activity in *Nkx3.1*; *Gpx3* knockout mice. (A) The ROS levels were measured in dorsal prostate of 4, 8, and 12 months *Nkx3.1*; *Gpx3* KO mice with DCFH-DA. Fluorescence spectrometer was used to determine ROS generation after staining with DCFH-DA (n=4~8). (B) The activity of antioxidant enzyme SOD was measured in dorsal prostate of 4, 8, and 12 months *Nkx3.1*; *Gpx3* KO mice (n=4~8). *P<0.05. Results are presented as means ± SEM. TP, total protein

3.5 *Gpx3* knockout increased hyperplasia of the prostate gland.

We analyzed the prostate of sacrificed mice histopathologically. As age increased, PIN with hyperplasia was observed in the prostate (Fig. 5A). Low-grade PIN was frequently observed in all 4-month-old mice and in 8- and 12-month-old *Nkx3.1*-/-; *Gpx3*+/+ mice. The papillary projection of the hyperplastic epithelium into the lumen of the gland was observed. Moderate-grade PIN was mainly observed in *Nkx3.1*-/-; *Gpx3*+/-, and *Nkx3.1*-/-; *Gpx3*-/- mice at 8 months of age. Like low-grade PIN, epithelial stratification was more frequently observed, with tall papillary projections filling the lumen. High-grade PIN was observed in *Nkx3.1*-/-; *Gpx3+/-*, and *Nkx3.1*-/-; *Gpx3*-/- mice at 12 months of age. Cell stratification and nuclear-to-cytoplasmic ratio were increased. Hyperplastic epithelium filled the lumen and formed a cribriform pattern. Histopathological scores were evaluated and an increase in the histopathologic score was observed in and *Nkx3.1*-/-; *Gpx3*-/- mice at 8 and 12 months of age (Fig. 5B). Epithelial thickness was measured and found to be increased in *Nkx3.1*-/-; *Gpx3*+/- and *Nkx3.1*-/-; *Gpx3*-/- mice at 8 and 12 months of age (Fig. 5C). Relative lumen area was also measured and observed to be decreased in *Nkx3.1*-/-; *Gpx3*+/- and *Nkx3.1*-/-; *Gpx3*-/- mice at 8 and 12 months of age (Fig. 5D).

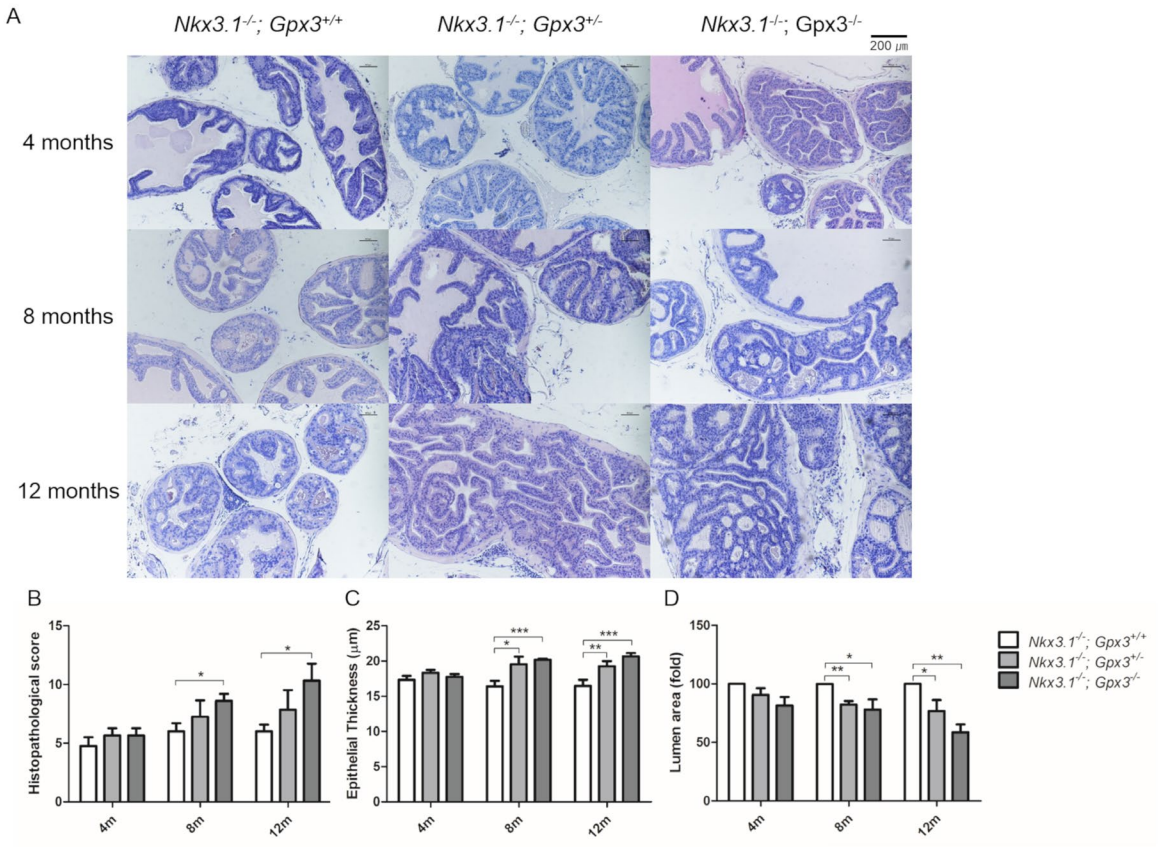

Fig. 5 Histopathological Analysis of prostate in *Nkx3.1*; *Gpx3* KO mice. (A) Representative images of H&E stained slides of prostate were taken (Magnification: 100x) (n=4~8). (B) Histopathologic score was evaluated in *Nkx3.1*; *Gpx3* KO mice as described before (n=4~8). (C) Epithelial thickness was measured in *Nkx3.1*; *Gpx3* KO mice with NIS-Elements BR 4.50.00 software (n=4~8). (D) Relative lumen area was measured in *Nkx3.1*; *Gpx3* KO mice (n=4~8). *P<0.05; **P<0.01; ***P<0.001. Results are presented as means ± SEM.

4 DISCUSSION

In our previous study, we found that a high-fat diet increased the progression of prostate cancer and decreased the expression of GPX3 in TRAMP mice (122). To further elucidate the relationship between GPX3 and prostate cancer, we obtained the cross of *Gpx3* knockout and TRAMP mice, and prostate cancer increased in *Gpx3* knockout groups (82). Based on these previous studies, it was hypothesized that GPX3 would play an important role in pre-cancerous PIN as well as in prostate cancer.

Loss of *Nkx3.1* plays an important role in the initiation of prostate cancer. Ouyang et al., reported an increase in oxidative stress in *Nkx3.1* knockout mice (87). In addition, the expression of antioxidant enzymes such as *Gpx2* and *Prdx6* was decreased and the expression of pro-oxidants such as *Qscn6* was increased. However, the expression of the antioxidant enzyme, *Gpx3*, was also increased, which was interpreted as a compensation for the loss of *Gpx2* and *Prdx6*. In the same experiment, when *Nkx3.1* and *Pten* were both knocked out, PIN progressed to invasive carcinoma, with decreased *Gpx3* expression. This means that GPX3 plays an important role in the transition of PIN to invasive carcinoma.

We measured basal levels of mRNA expression of *NKX3.1, GPX3* and ROS in normal prostate and prostate cancer cells. Reduced expression of *NKX3.1* and *GPX3* in cancer cells may be associated with increased ROS in cancer cells. We found that proliferation increased when RWPE-1 was treated with H_2O_2 to induce oxidative stress. This suggests that oxidative stress is associated with hyperplasia of normal prostate cells.

We crossed *Nkx3.1* knockout mice and *Gpx3* knockout mice to obtain double-knockout mice. In the overall findings, no significant differences could be identified. However, an increase in oxidative stress was observed in the prostates of *Gpx3* knockout mice, and the activity of the antioxidant enzyme SOD was decreased. This means that GPX3 plays an important role in the redox homeostasis of the prostate. We analyzed the expression of genes related to oxidative stress and found that the expression of antioxidant-related genes *Sod3, Gpx2, Hmox*, and *Cisd2* decreased. However, the expression of *Sod3, Hmox*, and *Cisd2* increased at 4 months of age, which is thought to be a compensation to suppress the oxidative stress caused by the loss of *Gpx3*. However, as the age increases, the expression of these genes appears to decrease with chronic oxidative stress.

We previously reported that loss of *Gpx3* in TRAMP mice increases Wnt/β-catenin signaling, leading to the development of prostate cancer (82). However, no change in these signals was observed in double-knockout mice. This suggests that Wnt/β-catenin signaling plays an important role in the development of invasive carcinoma, but other mechanisms are required to cause changes in the pre-cancerous PIN. Unfortunately, histopathological analysis revealed no invasive carcinoma. At 4 months of age, no change was observed in the *Gpx3* knockout mice. This is likely due to antioxidant-related genes, expressions of which increased as a compensation for the loss of Gpx3 at 4 months of age. However, after 8 months of age, lesions of PIN became more frequent and severe in *Gpx3* knockout mice. We confirmed that GPX3 enhanced hyperplasia of PIN histopathologically, although there was no drastic change in the prostate gland.

In this study, we confirmed that *Gpx3* loss increased the hyperplasia of PIN in the pre-cancerous stage of the prostate. Loss of *Gpx3* decreased the expression of genes related to antioxidant activity, induced oxidative stress, and decreased the activity of antioxidant enzymes. This means that GPX3 plays an important role in the transition of PIN to invasive carcinoma. Histopathologically, however, no invasive carcinoma was identified, and *Gpx3* loss did not increase Wnt/β-catenin signaling. Therefore, further research on the role of GPX3 in the transition of PIN to invasive carcinoma is needed.

GENERAL CONCLUSION

In this dissertation, I examined in detail how phloretin, pimozide and Gpx3-knockout affect redox homeostasis in prostate cancer. Prostate cancer is the most diagnosed non-skin cancer in US men and is a leading cause of cancer-related death. In 2019, 174,650 people will be diagnosed with prostate cancer in the US and 31,620 are expected to die. Prostate cancer is age-related, and increasing reactive oxygen species (ROS) play an important role in the development and progression of prostate cancer. ROS assists cancer cell proliferation, invasion and metastasis and inhibits apoptosis leading cancer progression.

In chapter I, I found that phloretin inhibits the growth of cancer cells by destroying redox homeostasis in prostate cancer. Phloretin, a type of flavonoid found mainly in apples, is known for its anti-cancer activity in addition to its antioxidant and anti-inflammatory effects. I treated phloretin in prostate cancer cell lines PC3 and DU145 to inhibit proliferation, colony formation and migration of cancer cells. Phloretin increased the production of ROS in prostate cancer and decreased the expression of SOD2, Catalase, Gpx1, Gpx3, and CISD2, which are associated with antioxidants. We also investigated the Wnt signaling pathway associated with increased ROS. The expression of Twist1, β-catenin, TCF4, FoxA2, and c-Myc was also reduced. Through this, I confirmed that phloretin suppressed prostate cancer by increasing ROS production and altering the expression of related antioxidant genes and Wnt signaling.

In chapter II, I confirmed *in vitro* and *in vivo* that pimozide, a psychotic drug, inhibits cancer by destroying redox homeostasis in prostate cancer as part of drug repurposing. Pimozide inhibited proliferation, colony formation and migration of prostate cancer cells. Pimozide increased ROS production in prostate cancer, which

was inhibited by GSH. Co-treatment of GSH inhibited the anticancer activity of pimozide. This means that ROS plays an important role in the anticancer activity of pimozide. DPI was treated to search for the source of ROS. DPI reduced ROS production, indicating that ROS production by pimozide is partly due to NADPH oxidase. Oxidative stress by pimozide altered the expression of oxidative stress-related genes, SOD1, Prdx6, Gpx2, and CISD2. The progression of prostate cancer was reduced when pimozide was administered to TRAMP mice with naturally occurring prostate cancer. Pathological scoring was decreased in the pimozide group, ROS production increased, and SOD activity decreased. This means that pimozide produced ROS *in vivo* and inhibited the formation of prostate cancer.

In chapter III, I found that inhibition of the antioxidant enzyme, *Gpx3*, reduced the hyperplasia of PIN, a precancerous stage of the prostate cancer. *Nkx3.1* knockout mice form PIN and are an important model for studying the early stages of prostate cancer. We created *Nkx3.1* and *Gpx3* double-knockout mice to see how *Gpx3* plays a role in PIN formation. Knockout of *Gpx3* altered the expression of oxidative stress-related genes, increased ROS production and decreased SOD activity. No change in Wnt signaling has been identified. Histopathological analysis showed that *Gpx3* knockout increased pathological scores, and hyperplasia was severe with increased epithelial thickness and decreased lumen area.

The roles of redox homeostasis in prostate cancer may depend on the stages of the cancer and the levels of oxidative stress. I observed changes in prostate cancer cell lines, TRAMP mice, and *Nkx3.1; Gpx3* KO mice by inducing oxidative stress, respectively. The treatment of phloretin and pimozide in cancer cell lines or TRAMP mice has been shown to inhibit cancer with oxidative stress. On the contrary, it was

confirmed that oxidative stress promoted progression to cancer at the precancerous stage in *Nkx3.1; Gpx3* KO mice. It is necessary to identify and access the roles of redox homeostasis according to the context of cancer. In this dissertation, I suggest that redox homeostasis of prostate cancer is an important target in understanding the biological, physiological and pathological characteristics of prostate cancer and in developing new anticancer strategies.

REFERENCES

1. Torre LA, Bray F, Siegel RL, Ferlay J, Lortet-Tieulent J, Jemal A. Global cancer statistics, 2012. CA: a cancer journal for clinicians. 2015;65(2):87-108.

2. Siegel RL, Miller KD, Jemal A. Cancer statistics, 2019. CA: a cancer journal for clinicians. 2019;69(1):7-34.

3. Khandrika L, Kumar B, Koul S, Maroni P, Koul HK. Oxidative stress in prostate cancer. Cancer letters. 2009;282(2):125-36.

4. Kim J, Kim J, Bae J-S. ROS homeostasis and metabolism: a critical liaison for cancer therapy. Experimental & Molecular Medicine. 2016;48(11):e269.

5. Boyer J, Liu RH. Apple phytochemicals and their health benefits. Nutrition journal. 2004;3(1):5.

6. Devi MA, Das N. In vitro effects of natural plant polyphenols on the proliferation of normal and abnormal human lymphocytes and their secretions of interleukin-2. Cancer letters. 1993;69(3):191-6.

7. Zhu S-P, Liu G, Wu X-T, Chen F-X, Liu J-Q, Zhou Z-H, et al. The effect of phloretin on human γδ T cells killing colon cancer SW-1116 cells. International immunopharmacology. 2013;15(1):6-14.

8. Nelson J, Falk R. The efficacy of phloridzin and phloretin on tumor cell growth. Anticancer research. 1992;13(6A):2287-92.

9. Egolf A, Coffey B. Current pharmacotherapeutic approaches for the treatment of Tourette syndrome. Drugs of today (Barcelona, Spain: 1998). 2014;50(2):159-79.

10. Nelson EA, Walker SR, Xiang M, Weisberg E, Bar-Natan M, Barrett R, et al. The STAT5 inhibitor pimozide displays efficacy in models of acute myelogenous leukemia driven by FLT3 mutations. Genes & cancer. 2012;3(7-8):503-11.

11. Krummel TM, Neifeld JP, Taub RN. Effects of dopamine agonists and antagonists on murine melanoma: correlation with dopamine binding activity. Cancer. 1982;49(6):1178-84.

12. Bertolesi GE, Shi C, Elbaum L, Jollimore C, Rozenberg G, Barnes S, et al. The Ca2+ channel antagonists mibefradil and pimozide inhibit cell growth via different cytotoxic mechanisms. Molecular pharmacology. 2002;62(2):210-9.

13. Strobl JS, Kirkwood KL, Lantz TK, Lewine MA, Peterson VA, Worley JF. Inhibition of human breast cancer cell proliferation in tissue culture by the neuroleptic agents pimozide and thioridazine. Cancer research. 1990;50(17):5399-405.

14. Zhou W, Chen M-K, Yu H-T, Zhong Z-H, Cai N, Chen G-Z, et al. The antipsychotic drug pimozide inhibits cell growth in prostate cancer through suppression of STAT3 activation. International journal of oncology. 2016;48(1):322-8.

15. Fako V, Yu Z, Henrich CJ, Ransom T, Budhu AS, Wang XW. Inhibition of wnt/β-catenin Signaling in Hepatocellular Carcinoma by an Antipsychotic Drug Pimozide. International journal of biological sciences. 2016;12(7):768.

16. Cai N, Zhou W, Ye L-L, Chen J, Liang Q-N, Chang G, et al. The STAT3 inhibitor pimozide impedes cell proliferation and induces ROS generation in human osteosarcoma by suppressing catalase expression. American journal of translational research. 2017;9(8):3853.

17. Taub R, Baker M. Treatment of metastatic malignant melanoma with pimozide. The Lancet. 1979;313(8116):605.

18. Chen J-J, Cai N, Chen G-Z, Jia C-C, Qiu D-B, Du C, et al. The neuroleptic drug pimozide inhibits stem-like cell maintenance and tumorigenicity in hepatocellular carcinoma. Oncotarget. 2017;8(11):17593.

19. Guyton K, Kensler TW. Oxidative mechanisms in carcinogenesis. British

medical bulletin. 1993;49(3):523-44.

20. Droge W. Free radicals in the physiological control of cell function. Physiological reviews. 2002;82(1):47-95.

21. Zhao H, Li J, Li X, Han C, Zhang Y, Zheng L, et al. Silencing GPX3 expression promotes tumor metastasis in human thyroid cancer. Current Protein and Peptide Science. 2015;16(4):316-21.

22. Peng D-F, Hu T-L, Schneider BG, Chen Z, Xu Z-K, El-Rifai W. Silencing of glutathione peroxidase 3 through DNA hypermethylation is associated with lymph node metastasis in gastric carcinomas. PLoS One. 2012;7(10):e46214.

23. Barrett CW, Ning W, Chen X, Smith JJ, Washington MK, Hill KE, et al. Tumor suppressor function of the plasma glutathione peroxidase gpx3 in colitis-associated carcinoma. Cancer research. 2013;73(3):1245-55.

24. Bostwick DG, Burke HB, Djakiew D, Euling S, Ho Sm, Landolph J, et al. Human prostate cancer risk factors. Cancer. 2004;101(S10):2371-490.

25. De Bont R, Van Larebeke N. Endogenous DNA damage in humans: a review of quantitative data. Mutagenesis. 2004;19(3):169-85.

26. Barzilai A, Rotman G, Shiloh Y. ATM deficiency and oxidative stress: a new dimension of defective response to DNA damage. DNA repair. 2002;1(1):3-25.

27. Naka K, Muraguchi T, Hoshii T, Hirao A. Regulation of reactive oxygen species and genomic stability in hematopoietic stem cells. Antioxidants & redox signaling. 2008;10(11):1883-94.

28. Lambeth JD. Nox enzymes, ROS, and chronic disease: an example of antagonistic pleiotropy. Free Radical Biology and Medicine. 2007;43(3):332-47.

29. Sauer H, Wartenberg M, Hescheler J. Reactive oxygen species as intracellular messengers during cell growth and differentiation. Cellular physiology and

biochemistry. 2001;11(4):173-86.

30. Finkel T. Signal transduction by mitochondrial oxidants. Journal of Biological Chemistry. 2012;287(7):4434-40.

31. Marengo B, Nitti M, Furfaro AL, Colla R, Ciucis CD, Marinari UM, et al. Redox homeostasis and cellular antioxidant systems: Crucial players in cancer growth and therapy. Oxidative Medicine and Cellular Longevity. 2016;2016.

32. Fuchs-Tarlovsky V. Role of antioxidants in cancer therapy. Nutrition. 2013;29(1):15-21.

33. Ziech D, Franco R, Georgakilas AG, Georgakila S, Malamou-Mitsi V, Schoneveld O, et al. The role of reactive oxygen species and oxidative stress in environmental carcinogenesis and biomarker development. Chemico-biological interactions. 2010;188(2):334-9.

34. Koppenol WH, Bounds PL, Dang CV. Otto Warburg's contributions to current concepts of cancer metabolism. Nature Reviews Cancer. 2011;11(5):325.

35. Tafani M, Sansone L, Limana F, Arcangeli T, De Santis E, Polese M, et al. The interplay of reactive oxygen species, hypoxia, inflammation, and sirtuins in cancer initiation and progression. Oxidative medicine and cellular longevity. 2016;2016.

36. Trachootham D, Alexandre J, Huang P. Targeting cancer cells by ROS-mediated mechanisms: a radical therapeutic approach? Nature reviews Drug discovery. 2009;8(7):579.

37. Ristow M, Schmeisser S. Extending life span by increasing oxidative stress. Free radical biology and medicine. 2011;51(2):327-36.

38. DeNicola GM, Karreth FA, Humpton TJ, Gopinathan A, Wei C, Frese K, et al. Oncogene-induced Nrf2 transcription promotes ROS detoxification and tumorigenesis. Nature. 2011;475(7354):106.

39. Tong L, Chuang C-C, Wu S, Zuo L. Reactive oxygen species in redox cancer therapy. Cancer letters. 2015;367(1):18-25.

40. Cairns RA, Harris IS, Mak TW. Regulation of cancer cell metabolism. Nature Reviews Cancer. 2011;11(2):85.

41. LeBleu VS, O'Connell JT, Herrera KNG, Wikman H, Pantel K, Haigis MC, et al. PGC-1α mediates mitochondrial biogenesis and oxidative phosphorylation in cancer cells to promote metastasis. Nature cell biology. 2014;16(10):992.

42. Klein EA, Thompson IM, Tangen CM, Crowley JJ, Lucia MS, Goodman PJ, et al. Vitamin E and the risk of prostate cancer: the Selenium and Vitamin E Cancer Prevention Trial (SELECT). Jama. 2011;306(14):1549-56.

43. Padayatty SJ, Riordan HD, Hewitt SM, Katz A, Hoffer LJ, Levine M. Intravenously administered vitamin C as cancer therapy: three cases. Cmaj. 2006;174(7):937-42.

44. Greenlee H, Kwan ML, Kushi LH, Song J, Castillo A, Weltzien E, et al. Antioxidant supplement use after breast cancer diagnosis and mortality in the Life After Cancer Epidemiology (LACE) cohort. Cancer. 2012;118(8):2048-58.

45. Jeon D, Jeong M-C, Jnawali HN, Kwak C, Ryoo S, Jung ID, et al. Phloretin Exerts Anti-Tuberculosis Activity and Suppresses Lung Inflammation. Molecules. 2017;22(1):183.

46. Crespy V, Aprikian O, Morand C, Besson C, Manach C, Demigné C, et al. Bioavailability of phloretin and phloridzin in rats. The Journal of nutrition. 2001;131(12):3227-30.

47. PARPINELLO GP, VERSARI A, GALASSI S. Phloretin glycosides: bioactive compounds in apple fruit, purees, and juices. Journal of medicinal food. 2000;3(3):149-51.

48. Rezk BM, Haenen GR, van der Vijgh WJ, Bast A. The antioxidant activity of phloretin: the disclosure of a new antioxidant pharmacophore in flavonoids. Biochemical and biophysical research communications. 2002;295(1):9-13.

49. Stangl V, Lorenz M, Ludwig A, Grimbo N, Guether C, Sanad W, et al. The flavonoid phloretin suppresses stimulated expression of endothelial adhesion molecules and reduces activation of human platelets. The Journal of nutrition. 2005;135(2):172-8.

50. Chang W-T, Huang W-C, Liou C-J. Evaluation of the anti-inflammatory effects of phloretin and phlorizin in lipopolysaccharide-stimulated mouse macrophages. Food chemistry. 2012;134(2):972-9.

51. Yang KC, Tsai CY, Wang YJ, Wei PL, Lee CH, Chen JH, et al. Apple polyphenol phloretin potentiates the anticancer actions of paclitaxel through induction of apoptosis in human hep G2 cells. Molecular carcinogenesis. 2009;48(5):420-31.

52. Lin S-T, Tu S-H, Yang P-S, Hsu S-P, Lee W-H, Ho C-T, et al. Apple polyphenol phloretin inhibits colorectal cancer cell growth via inhibition of the type 2 glucose transporter and activation of p53-mediated signaling. Journal of agricultural and food chemistry. 2016;64(36):6826-37.

53. Wu CH, Ho YS, Tsai CY, Wang YJ, Tseng H, Wei PL, et al. In vitro and in vivo study of phloretin-induced apoptosis in human liver cancer cells involving inhibition of type II glucose transporter. International journal of cancer. 2009;124(9):2210-9.

54. Liu Y, Fan C, Pu L, Wei C, Jin H, Teng Y, et al. Phloretin induces cell cycle arrest and apoptosis of human glioblastoma cells through the generation of reactive oxygen species. Journal of neuro-oncology. 2016;128(2):217-23.

55. Boguski MS, Mandl KD, Sukhatme VP. Repurposing with a difference. Science. 2009;324(5933):1394-5.

56. Carley DW. Drug repurposing: identify, develop and commercialize new uses for existing or abandoned drugs. Part I. IDrugs: the investigational drugs journal. 2005;8(4):306.

57. Carley DW. Drug repurposing: identify, develop and commercialize new uses for existing or abandoned drugs. Part II. IDrugs: the investigational drugs journal. 2005;8(4):310.

58. Blatt J, Corey SJ. Drug repurposing in pediatrics and pediatric hematology oncology. Drug discovery today. 2013;18(1-2):4-10.

59. Sleire L, Førde HE, Netland IA, Leiss L, Skeie BS, Enger PØ. Drug repurposing in cancer. Pharmacological research. 2017;124:74-91.

60. Kasznicki J, Sliwinska A, Drzewoski J. Metformin in cancer prevention and therapy. Annals of translational medicine. 2014;2(6).

61. Triscott J, Lee C, Hu K, Fotovati A, Berns R, Pambid M, et al. Disulfiram, a drug widely used to control alcoholism, suppresses self-renewal of glioblastoma and overrides resistance to temozolomide. Oncotarget. 2012;3(10):1112.

62. Saponara M, Pantaleo MA, Nannini M, Biasco G. Treatments for gastrointestinal stromal tumors that are resistant to standard therapies. Future Oncology. 2014;10(13):2045-59.

63. Kelley R, Hwang J, Magbanua M, Watt L, Beumer J, Christner S, et al. A phase 1 trial of imatinib, bevacizumab, and metronomic cyclophosphamide in advanced colorectal cancer. British journal of cancer. 2013;109(7):1725.

64. Nelson EA, Walker SR, Weisberg E, Bar-Natan M, Barrett R, Gashin LB, et al. The STAT5 inhibitor pimozide decreases survival of chronic myelogenous leukemia cells resistant to kinase inhibitors. Blood. 2011;117(12):3421-9.

65. Kypta RM, Waxman J. Wnt/β-catenin signalling in prostate cancer. Nature

Reviews Urology. 2012;9(8):418-28.

66. Burk RF, Olson GE, Winfrey VP, Hill KE, Yin D. Glutathione peroxidase-3 produced by the kidney binds to a population of basement membranes in the gastrointestinal tract and in other tissues. American Journal of Physiology-Gastrointestinal and Liver Physiology. 2011;301(1):G32-G8.

67. Chu F-F, Esworthy RS, Doroshow J, Doan K, Liu X-F. Expression of plasma glutathione peroxidase in human liver in addition to kidney, heart, lung, and breast in humans and rodents. Blood. 1992;79(12):3233-8.

68. Takebe G, Yarimizu J, Saito Y, Hayashi T, Nakamura H, Yodoi J, et al. A comparative study on the hydroperoxide and thiol specificity of the glutathione peroxidase family and selenoprotein P. Journal of Biological Chemistry. 2002;277(43):41254-8.

69. Wang H, Luo K, Tan L-Z, Ren B-G, Gu L-Q, Michalopoulos G, et al. p53-induced gene 3 mediates cell death induced by glutathione peroxidase 3. Journal of Biological Chemistry. 2012;287(20):16890-902.

70. An BC, Choi Y-D, Oh I-J, Kim JH, Park J-I, Lee S-w. GPx3-mediated redox signaling arrests the cell cycle and acts as a tumor suppressor in lung cancer cell lines. PloS one. 2018;13(9):e0204170.

71. Kohler BA, Sherman RL, Howlader N, Jemal A, Ryerson AB, Henry KA, et al. Annual report to the nation on the status of cancer, 1975-2011, featuring incidence of breast cancer subtypes by race/ethnicity, poverty, and state. Journal of the National Cancer Institute. 2015;107(6):djv048.

72. Center MM, Jemal A, Lortet-Tieulent J, Ward E, Ferlay J, Brawley O, et al. International variation in prostate cancer incidence and mortality rates. European urology. 2012;61(6):1079-92.

73. Korswagen HC. Regulation of the Wnt/β-catenin pathway by redox signaling. Developmental cell. 2006;10(6):687-8.

74. Yu X, Wang Y, Jiang M, Bierie B, Roy-Burman P, Shen MM, et al. Activation of β-Catenin in mouse prostate causes HGPIN and continuous prostate growth after castration. The Prostate. 2009;69(3):249-62.

75. Miller JR. The wnts. Genome biology. 2001;3(1):reviews3001. 1.

76. Chesire DR, Ewing CM, Gage WR, Isaacs WB. In vitro evidence for complex modes of nuclear β-catenin signaling during prostate growth and tumorigenesis. Oncogene. 2002;21(17):2679.

77. Shin SY, Kim CG, Jho E-H, Rho M-S, Kim YS, Kim Y-H, et al. Hydrogen peroxide negatively modulates Wnt signaling through downregulation of β-catenin. Cancer letters. 2004;212(2):225-31.

78. Kypta RM, Waxman J. Wnt/β-catenin signalling in prostate cancer. Nature Reviews Urology. 2012;9(8):418.

79. Prasannaraj G, Sahi SV, Benelli G, Venkatachalam P. Coating with Active Phytomolecules Enhances Anticancer Activity of Bio-Engineered Ag Nanocomplex. Journal of Cluster Science. 2017;28(4):2349-67.

80. Priyadharshini RI, Prasannaraj G, Geetha N, Venkatachalam P. Microwave-mediated extracellular synthesis of metallic silver and zinc oxide nanoparticles using macro-algae (Gracilaria edulis) extracts and its anticancer activity against human PC3 cell lines. Applied biochemistry and biotechnology. 2014;174(8):2777-90.

81. Meyer F, Galan P, Douville P, Bairati I, Kegle P, Bertrais S, et al. Antioxidant vitamin and mineral supplementation and prostate cancer prevention in the SU. VI. MAX trial. International journal of cancer. 2005;116(2):182-6.

82. Chang SN, Lee JM, Oh H, Park JH. Glutathione peroxidase 3 inhibits prostate

tumorigenesis in TRAMP mice. The Prostate. 2016;76(15):1387-98.

83. Lill R. Function and biogenesis of iron–sulphur proteins. Nature. 2009;460(7257):831.

84. Chen Y-F, Kao C-H, Chen Y-T, Wang C-H, Wu C-Y, Tsai C-Y, et al. Cisd2 deficiency drives premature aging and causes mitochondria-mediated defects in mice. Genes & development. 2009;23(10):1183-94.

85. Chang NC, Nguyen M, Bourdon J, Risse P-A, Martin J, Danialou G, et al. Bcl-2-associated autophagy regulator Naf-1 required for maintenance of skeletal muscle. Human molecular genetics. 2012;21(10):2277-87.

86. Li S-M, Chen C-H, Chen Y-W, Yen Y-C, Fang W-T, Tsai F-Y, et al. Upregulation of CISD2 augments ROS homeostasis and contributes to tumorigenesis and poor prognosis of lung adenocarcinoma. Scientific reports. 2017;7(1):11893.

87. Ouyang X, DeWeese TL, Nelson WG, Abate-Shen C. Loss-of-function of Nkx3. 1 promotes increased oxidative damage in prostate carcinogenesis. Cancer research. 2005;65(15):6773-9.

88. Prendergast GC. Mechanisms of apoptosis by c-Myc. Oncogene. 1999;18(19):2967.

89. Cassinelli G, Supino R, Zuco V, Lanzi C, Scovassi AI, Semple SC, et al. Role of c-myc protein in hormone refractory prostate carcinoma: cellular response to paclitaxel. Biochemical pharmacology. 2004;68(5):923-31.

90. Li Q, Dang CV. c-Myc overexpression uncouples DNA replication from mitosis. Molecular and cellular biology. 1999;19(8):5339-51.

91. Gajula RP, Chettiar ST, Williams RD, Thiyagarajan S, Kato Y, Aziz K, et al. The twist box domain is required for Twist1-induced prostate cancer metastasis. Molecular Cancer Research. 2013:molcanres. 0218.2013.

92. Whitburn J, Edwards CM, Sooriakumaran P. Metformin and prostate cancer: a new role for an old drug. Current urology reports. 2017;18(6):46.

93. Lin J, Haffner MC, Zhang Y, Lee BH, Brennen WN, Britton J, et al. Disulfiram is a DNA demethylating agent and inhibits prostate cancer cell growth. The Prostate. 2011;71(4):333-43.

94. Adaramoye O, Erguen B, Oyebode O, Nitzsche B, Höpfner M, Jung K, et al. Antioxidant, antiangiogenic and antiproliferative activities of root methanol extract of Calliandra portoricensis in human prostate cancer cells. Journal of integrative medicine. 2015;13(3):185-93.

95. Kim U, Kim C-Y, Lee JM, Oh H, Ryu B, Kim J, et al. Phloretin Inhibits the Human Prostate Cancer Cells Through the Generation of Reactive Oxygen Species. Pathology & Oncology Research. 2019:1-8.

96. Park J-H, Walls JE, Galvez JJ, Kim M, Abate-Shen C, Shen MM, et al. Prostatic Intraepithelial Neoplasia in Genetically Engineered Mice. The American Journal of Pathology. 2002;161(2):727-35.

97. Berman-Booty LD, Sargeant AM, Rosol TJ, Rengel RC, Clinton SK, Chen CS, et al. A review of the existing grading schemes and a proposal for a modified grading scheme for prostatic lesions in TRAMP mice. Toxicol Pathol. 2012;40(1):5-17.

98. Shao B, Zhu L, Dong M, Wang J, Wang J, Xie H, et al. DNA damage and oxidative stress induced by endosulfan exposure in zebrafish (Danio rerio). Ecotoxicology. 2012;21(5):1533-40.

99. D'Autréaux B, Toledano MB. ROS as signalling molecules: mechanisms that generate specificity in ROS homeostasis. Nature reviews Molecular cell biology. 2007;8(10):813.

100. Kaplan-Lefko PJ, Chen TM, Ittmann MM, Barrios RJ, Ayala GE, Huss WJ, et

al. Pathobiology of autochthonous prostate cancer in a pre-clinical transgenic mouse model. The Prostate. 2003;55(3):219-37.

101. Xiao D, Powolny AA, Moura MB, Kelley EE, Bommareddy A, Kim S-H, et al. Phenethyl isothiocyanate inhibits oxidative phosphorylation to trigger reactive oxygen species-mediated death of human prostate cancer cells. Journal of Biological Chemistry. 2010;285(34):26558-69.

102. Wu X, Gong S, Roy-Burman P, Lee P, Culig Z. Current mouse and cell models in prostate cancer research. Endocrine-related cancer. 2013;20(4):R155-R70.

103. Jayakumar S, Kunwar A, Sandur SK, Pandey BN, Chaubey RC. Differential response of DU145 and PC3 prostate cancer cells to ionizing radiation: role of reactive oxygen species, GSH and Nrf2 in radiosensitivity. Biochimica et Biophysica Acta (BBA)-General Subjects. 2014;1840(1):485-94.

104. Poillet-Perez L, Despouy G, Delage-Mourroux R, Boyer-Guittaut M. Interplay between ROS and autophagy in cancer cells, from tumor initiation to cancer therapy. Redox biology. 2015;4:184-92.

105. He WW, Sciavolino PJ, Wing J, Augustus M, Hudson P, Meissner PS, et al. A novel human prostate-specific, androgen-regulated homeobox gene (NKX3. 1) that maps to 8p21, a region frequently deleted in prostate cancer. Genomics. 1997;43(1):69-77.

106. Korkmaz KS, Korkmaz CG, Ragnhildstveit E, Kizildag S, Pretlow TG, Saatcioglu F. Full-length cDNA sequence and genomic organization of human NKX3A—alternative forms and regulation by both androgens and estrogens. Gene. 2000;260(1-2):25-36.

107. Asatiani E, Huang W-X, Wang A, Ortner ER, Cavalli LR, Haddad BR, et al. Deletion, methylation, and expression of the NKX3. 1 suppressor gene in primary

human prostate cancer. Cancer research. 2005;65(4):1164-73.

108. Vocke CD, Pozzatti RO, Bostwick DG, Florence CD, Jennings SB, Strup SE, et al. Analysis of 99 microdissected prostate carcinomas reveals a high frequency of allelic loss on chromosome 8p12–21. Cancer research. 1996;56(10):2411-6.

109. Bhatia-Gaur R, Donjacour AA, Sciavolino PJ, Kim M, Desai N, Young P, et al. Roles for Nkx3. 1 in prostate development and cancer. Genes & development. 1999;13(8):966-77.

110. Tanaka M, Komuro I, Inagaki H, Jenkins NA, Copeland NG, Izumo S. Nkx3. 1, a murine homolog of Drosophila bagpipe, regulates epithelial ductal branching and proliferation of the prostate and palatine glands. Developmental dynamics: an official publication of the American Association of Anatomists. 2000;219(2):248-60.

111. Abdulkadir SA, Magee JA, Peters TJ, Kaleem Z, Naughton CK, Humphrey PA, et al. Conditional loss of Nkx3. 1 in adult mice induces prostatic intraepithelial neoplasia. Molecular and cellular biology. 2002;22(5):1495-503.

112. Abate-Shen C, Banach-Petrosky WA, Sun X, Economides KD, Desai N, Gregg JP, et al. Nkx3. 1; Pten mutant mice develop invasive prostate adenocarcinoma and lymph node metastases. Cancer research. 2003;63(14):3886-90.

113. Chu F-F, Doroshow J, and, Esworthy R. Expression, characterization, and tissue distribution of a new cellular selenium-dependent glutathione peroxidase, GSHPx-GI. Journal of Biological Chemistry. 1993;268(4):2571-6.

114. Grabowska MM, DeGraff DJ, Yu X, Jin RJ, Chen Z, Borowsky AD, et al. Mouse models of prostate cancer: picking the best model for the question. Cancer Metastasis Rev. 2014;33(2-3):377-97.

115. Olson GE, Whitin JC, Hill KE, Winfrey VP, Motley AK, Austin LM, et al. Extracellular glutathione peroxidase (Gpx3) binds specifically to basement

membranes of mouse renal cortex tubule cells. American Journal of Physiology-Renal Physiology. 2010;298(5):F1244-F53.

116. Lawler JM, Song W, Demaree SR. Hindlimb unloading increases oxidative stress and disrupts antioxidant capacity in skeletal muscle. Free radical biology and medicine. 2003;35(1):9-16.

117. Bowen C, Bubendorf L, Voeller HJ, Slack R, Willi N, Sauter G, et al. Loss of NKX3. 1 Expression in Human Prostate Cancers Correlates with Tumor Progression1, 2. Cancer research. 2000;60(21):6111-5.

118. Yan PY, Yu G, Tseng G, Cieply K, Nelson J, Defrances M, et al. Glutathione peroxidase 3, deleted or methylated in prostate cancer, suppresses prostate cancer growth and metastasis. Cancer research. 2007;67(17):8043-50.

119. Kipp AP. Selenium-dependent glutathione peroxidases during tumor development. Advances in cancer research. 136: Elsevier; 2017. p. 109-38.

120. Udensi UK, Tchounwou PB. Oxidative stress in prostate hyperplasia and carcinogenesis. Journal of Experimental & Clinical Cancer Research. 2016;35(1):139.

121. Wartenberg M, Schallenberg M, Hescheler J, Sauer H. Reactive oxygen species-mediated regulation of eNOS and iNOS expression in multicellular prostate tumor spheroids. International journal of cancer. 2003;104(3):274-82.

122. Chang SN, Han J, Abdelkader TS, Kim TH, Lee JM, Song J, et al. High animal fat intake enhances prostate cancer progression and reduces glutathione peroxidase 3 expression in early stages of TRAMP mice. Prostate. 2014;74(13):1266-77.

국문 초록

전립선 암에서 암의 단계와 산화 스트레스 수준에 따른 산화환원항상성의 역할

김욱진

서울대학교 대학원

수의병인생물학 및 예방수의학 전공 (실험동물의학)

(지도교수: 박재학)

전립선 암은 선진국 남성에서 가장 많이 진단된 비-피부암이며 암 관련 사망의 주요 원인이다. 전립선 암은 연령과 관련이 있으며, 연령에 따라 증가하는 활성산소 (ROS)와 관련된 신호 경로는 암의 발달과 진행에 중요한 역할을 한다. 활성산소는 세포 증식, 침습 및 전이를 촉진하는 한편, 세포자멸사를 억제하여 암 진행을 초래한다. 그에 따라, 항산화 효과에 기반한 항암제들이 보고되었다. 그러나, 더

높은 수준의 활성산소는 세포주기 정지, 세포자멸사 및 괴사를 유발하여 암을 억제한다. 전립선 암에서 활성산소의 역할에 대해서는 아직 많이 알려져 있지 않다.

제1장의 연구에서, 폴리페놀의 일종인 phloretin은 산화 스트레스를 유발하여 전립선 암 세포 PC3와 DU145를 억제했다. 이 연구에서 전립선 암 세포 PC3와 DU145에서 phloretin을 처리한 후 암 세포의 증식, 집락 형성 및 세포 이동의 변화를 확인했다. 활성산소와 관련된 유전자 발현 양의 변화를 측정하였다. phloretin은 활성산소를 증가시키고 두 세포주 모두에서 세포 증식, 집락 형성, 세포 이동을 억제하였다. 또한, phloretin을 처리하자, 항산화 효소 (Catalase, SOD2, Gpx1, Gpx3)의 유전자 발현 량이 감소하면서, 산화 스트레스를 증가시켰다. 또한, 위 유전자들의 조절 인자 CISD2의 발현도 감소되었다. 또한, 증가한 활성산소는 Wnt/β-catenin 신호 전달 경로 (β-catenin, TCF4, FoxA2, c-Myc) 및 Twist1의 유전자 발현 량을 상당히 감소시킨 것을 발견하였다. 따라서, phloretin은 Wnt/β-catenin 신호에 영향을 주는 활성산소를 생성하여 암을 억제한다. 이 연구의 결과에 따르면, phloretin은 *in vitro* 상에서 전립선 암에 치료 효과가 있어 암 세포주 PC3 및 DU145의 증식 및 이동을 억제하였다. Phloretin의 메커니즘은 활성산소의 생산에 기인하는 것으로 생각된다. 유망한 항암제로서 phloretin의 가능성을 확인하였다.

제2장에서는 이미 다른 목적으로 승인된 약물의 항암 능력을 평가하여 새로운 약물을 발견하기 위한 약물 용도 변경에 중점을 두었다. 제2장은 FDA의 승인을 받은 항정신병약인 pimozide가 전립선 암에서 산화 스트레스를 유도함으로써 *in vitro* 및 *in vivo*에서 전립선 암을 억제하는 것을 보고했다. Pimozide를 전립선 암 세포, PC3와 DU145에 처치 후, 세포 증식, 집락 형성, 세포 이동, 활성산소 생산 및 항 산화 스트레스 관련 유전자의 발현량을 조사했다. 또한, 전립선 암이 있는 유전자변형 마우스인 TRAMP에 pimozide를 투여 후 조직병리학적 분석, 활성산소 생성 및 SOD 활성 분석을 하였다. Pimozide는 두 세포주 모두에서 활성산소 생성을 증가시켰으며 세포 증식, 집락 형성, 세포 이동을 억제했다. Pimozide에 의해 유도된 산화 스트레스는 항산화 효소 (SOD1, Prdx6, Gpx2) 및 CISD2의 발현을 변화시켰다. 항산화 물질인 GSH를 같이 처리하자 pimozide로 유도된 활성산소의 양이 감소했으며, 세포 증식의 억제가 감소하였다. TRAMP 마우스에 pimozide를 투여하자, 활성산소 생성이 증가하고 SOD 활성이 감소하면서 전립선 암의 진행을 감소시켰다. 위의 결과는 항정신병 약물인 pimozide가 *in vitro* 및 *in vivo* 상에서 전립선 암을 억제한다는 것을 시사한다. Pimozide의 메커니즘은 활성산소 생성 증가와 관련이 있을 수 있으며, pimozide는 유망한 항암제로서의 가능성이 있다.

제1장과 제2장은 항암 효과를 지닌 물질이 전립선 암 세포와 TRAMP 마우

스에서 산화 스트레스를 유발하여 전립선 암을 억제한다고 보고하였다. 제3장에서는 선천적으로 손상된 산화환원항상성이 유전자 변형 마우스에서 전립선 암의 전암 단계에 어떤 영향을 미치는지 연구했다. Glutathione peroxidase 3 (*GPX3*)는 산화 스트레스로부터 세포를 보호하고 인간 전립선 암에 발현이 감소한다고 보고되었다. 우리는 이전에 *Gpx3*의 감소가 TRAMP 마우스에서 전립선 암을 증가시키는 것을 확인하였고 Gpx3가 전립선의 전암 단계인 prostatic Intraepithelial neoplasia (PIN)의 발달에 중요한 역할을 할 수 있다고 가정했다. 이중 녹아웃 마우스 *Nkx3.1*$^{-/-}$; *Gpx3*$^{+/+}$, *Nkx3.1*$^{-/-}$; *Gpx3*$^{+/-}$ 및 *Nkx3.1*$^{-/-}$; *Gpx3*$^{-/-}$가 생산되었다. 무작위로 그룹을 나눈 동물을 4, 8, 12개월에 안락사 후 체중과 비뇨생식관 (GUT) 무게를 측정하였다. 전립선에서 산화 스트레스 및 Wnt 신호 전달과 관련된 유전자의 발현을 분석하였다. 또한 병리조직학적 분석과 활성산소 및 SOD 활성을 측정하였다.. Gpx3의 발현량의 감소는 *Nkx3.1* 녹아웃 마우스에서 체중 및 비뇨생식관 중량에 유의미한 영향을 미치지 않았다. 산화 스트레스와 관련된 *Sod3, Nos2, Hmox, Cisd2*의 mRNA 발현은 4개월령 *Nkx3.1*$^{-/-}$; *Gpx3*$^{-/-}$ 마우스에서 유의하게 증가하였으나, 8개월과 12개월에서는 유의적으로 감소하였다. Wnt 신호 전달과 관련된 *Ctnnb1* 및 하위 신호에는 유의미한 변화가 없었다. 12개월령 Nkx3.1$^{-/-}$; Gpx3$^{-/-}$ 마우스에서 증가한 ROS와 감소한 SOD 활성이 관찰되었다. *Gpx3* 녹아웃 마우스에서 조직병리학적 점수와 상

피세포의 두께가 증가하였고 전립선의 내강 면적이 감소하였다. 이번 실험의 결과는 항산화 효소인 *Gpx3*가 전립선의 초기 전암 단계인 PIN에서 전립선 세포의 증식을 억제하는 역할을 한다는 것을 *in vivo* 상에서 처음으로 보고하였다.

전립선 암에서 산화환원항상성의 역할은 암의 단계와 산화 스트레스 수준에 따라 다를 수 있다. 나는 전립선 암 세포주, TRAMP 마우스, *Nkx3.1; Gpx3* 녹아웃 마우스에 산화 스트레스를 유발하여 변화를 관찰하였다. Phloretin과 pimozide는 암세포와 TRAMP 마우스에서 산화 스트레스를 유발하여 암을 억제하는 것을 보여주었다. 그와 반대로, *Nkx3.1; Gpx3* 녹아웃 마우스의 전암 단계에선 산화 스트레스가 암으로의 진행을 촉진하는 것을 확인하였다. 산화환원항상성의 역할을 이해하고 접근하기 위해서는 암의 맥락을 이해하는 것이 필요하다. 전립선 암의 생물학적, 생리학적, 병리학적 특징을 이해하고 새로운 항암 신약 개발 전략을 위해선 산화환원항상성의 역할을 이해하는 것이 중요하다.

주요어: 전립선 암, 산화 스트레스, 활성산소 (ROS), 항암, *Gpx3*

학번: 2016-21761